U.S. DEPARTMENT OF COMMERCE
National Technical Information Service

PB-290 945

High-Gradient Magnetic Separation for Removal of Sulfur from Coal

General Electric Corporate Research and Development, Schenectady, NY

Prepared for

Industrial Environmental Research Lab, Research Triangle Park, NC

Nov 78

PB 290945

DoE

United States
Department of Energy

Division of Solid Fuel
Mining and Preparation
Pittsburgh PA 15213

FE-8969-1

EPA

U.S. Environmental Protection Agency
Office of Research and Development

Industrial Environmental Research
Laboratory
Research Triangle Park NC 27711

EPA-600/7-78-208
November 1978

High-gradient Magnetic Separation for Removal of Sulfur from Coal

Interagency Energy/Environment R&D Program Report

FEB 15 1979

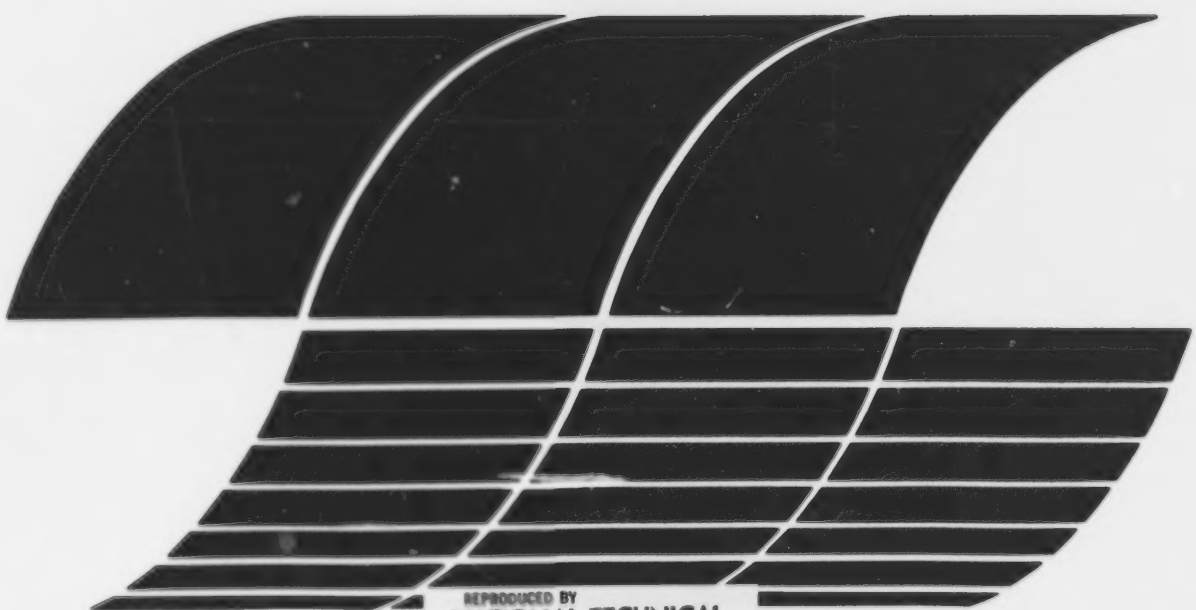

REPRODUCED BY
NATIONAL TECHNICAL
INFORMATION SERVICE
U. S. DEPARTMENT OF COMMERCE
SPRINGFIELD, VA. 22161

RESEARCH REPORTING SERIES

Research reports of the Office of Research and Development, U.S. Environmental Protection Agency, have been grouped into nine series. These nine broad categories were established to facilitate further development and application of environmental technology. Elimination of traditional grouping was consciously planned to foster technology transfer and a maximum interface in related fields. The nine series are:

1. Environmental Health Effects Research
2. Environmental Protection Technology
3. Ecological Research
4. Environmental Monitoring
5. Socioeconomic Environmental Studies
6. Scientific and Technical Assessment Reports (STAR)
7. Interagency Energy-Environment Research and Development
8. "Special" Reports
9. Miscellaneous Reports

This report has been assigned to the INTERAGENCY ENERGY-ENVIRONMENT RESEARCH AND DEVELOPMENT series. Reports in this series result from the effort funded under the 17-agency Federal Energy/Environment Research and Development Program. These studies relate to EPA's mission to protect the public health and welfare from adverse effects of pollutants associated with energy systems. The goal of the Program is to assure the rapid development of domestic energy supplies in an environmentally-compatible manner by providing the necessary environmental data and control technology. Investigations include analyses of the transport of energy-related pollutants and their health and ecological effects; assessments of, and development of, control technologies for energy systems; and integrated assessments of a wide range of energy-related environmental issues.

EPA REVIEW NOTICE

This report has been reviewed by the participating Federal Agencies, and approved for publication. Approval does not signify that the contents necessarily reflect the views and policies of the Government, nor does mention of trade names or commercial products constitute endorsement or recommendation for use.

This document is available to the public through the National Technical Information Service, Springfield, Virginia 22161.

Printed in the United States of America
USDOE Technical Information Center, Oak Ridge, Tennessee

TECHNICAL REPORT DATA
(Please read Instructions on the reverse before completing)

1. REPORT NO.	2.	3. RECIPIENT'S ACCESSION NO.
FE-8969-1(EPA-600/7-78-208)		PB 290945

4. TITLE AND SUBTITLE	5. REPORT DATE
High-gradient Magnetic Separation for Removal of Sulfur from Coal	November 1978
	6. PERFORMING ORGANIZATION CODE
7. AUTHOR(S)	8. PERFORMING ORGANIZATION REPORT NO.
F.E. Luborsky	
9. PERFORMING ORGANIZATION NAME AND ADDRESS	10. PROGRAM ELEMENT NO.
General Electric Company Corporate Research and Development PO Box 8 Schnectady, New York 12301	EHE623A
	11. CONTRACT/GRANT NO.
	EPA Interagency Agreement DXE 685 AK
12. SPONSORING AGENCY NAME AND ADDRESS	13. TYPE OF REPORT AND PERIOD COVERED
EPA, Office of Research and Development Industrial Environmental Research Laboratory Research Triangle Park, NC 27711	Final; 3/76-7/77
	14. SPONSORING AGENCY CODE
	EPA/600/13

15. SUPPLEMENTARY NOTES IERL-RTP project officer is David A. Kirchgessner, MD-61, 919/541-2851. DoE project officer is R.E. Hucko, Div. of Solid Fuel Mining and Preparation, Pittsburgh PA 15213.

16. ABSTRACT The report gives results of a thorough physical, chemical, and magnetic characterization of a Pennsylvania coal from the Upper Freeport seam. The powdered coal was then subjected to high-gradient magnetic separations, as a function of magnetic field and fluid velocity, in both a water slurry and an air dispersion. Ash and pyritic sulfur reductions occurred with increasing magnetic field intensities and decreasing fluid velocities. The best results were obtained in water slurries where approximately 50 percent of the total sulfur and 50 percent of the ash were removed. Air dispersions produced insignificant results.

17. KEY WORDS AND DOCUMENT ANALYSIS

a. DESCRIPTORS	b. IDENTIFIERS/OPEN ENDED TERMS	c. COSATI Field/Group
Pollution	Pollution Control	13B
Coal	Stationary Sources	08G/21D
Desulfurization	High-gradient Magnetic Separation	07A/07D
Magnetic Separators		13I
Separation		
Magnetic Properties		20C

18. DISTRIBUTION STATEMENT	19. SECURITY CLASS (This Report)	21. NO. OF PAGES
Unlimited	Unclassified	90
	20. SECURITY CLASS (This page)	22. PRICE
	Unclassified	A05-A01

EPA Form 2220-1 (9-73)

FE-8969-1
(EPA-600/7-78-208)
November 1978
Distribution Category UC-90b

High-gradient Magnetic Separation for Removal of Sulfur from Coal

by

F.E. Luborsky

General Electric Company
Corporate Research and Development
P.O. Box 8
Schnectady, New York 12301

EPA/DoE Interagency Agreement No. DXE685AK
Program Element No. EHE623A

EPA Project Officer: David A. Kirchgessner

Industrial Environmental Research Laboratory
Research Triangle Park, NC 27711

DoE Project Officer: Richard E. Hucko

Division of Solid Fuel Mining and Preparation
Pittsburgh, PA 15213

Prepared for

U.S. ENVIRONMENTAL PROTECTION AGENCY
Office of Research and Development
Washington, DC 20460

and

U.S. DEPARTMENT OF ENERGY
Division of Solid Fuel Mining and Preparation
Pittsburgh, PA 15213

ia

HIGH GRADIENT MAGNETIC SEPARATION FOR REMOVAL OF SULFUR FROM COAL

F. E. Luborsky

FINAL REPORT

Period Covered: March 1, 1976 through January 31, 1977

Contract No. HO366008

BUREAU OF MINES
U. S. DEPARTMENT OF THE INTERIOR
PITTSBURGH, PENNSYLVANIA

February 1977

General Electric Company
Corporate Research and Development
Schenectady, New York

ib

ABSTRACT

In this project a Pennsylvania coal from the Upper Freeport seam was thoroughly characterized physically, chemically, and magnetically. The powdered coal was then subjected to high gradient magnetic separations, as a function of magnetic field and fluid velocity, in both a water slurry and an air dispersion.

Ash and pyritic sulfur reductions occurred with increasing magnetic field intensities and decreasing fluid velocities. The best results were obtained in water slurries where approximately fifty percent of the total sulfur and fifty percent of the ash were removed. Air dispersions produced insignificant results.

TABLE OF CONTENTS

Section		Page
I	SUMMARY	1-1
II	INTRODUCTION	2-1
	Objective	2-1
	Background	2-1
	Previous Work on Magnetic Desulfurization of Coal	2-1
III	MAGNETIC SEPARATOR MODELING THEORY	3-1
	Theoretical Analysis	3-1
	Calculations for Ribbon-Like Fibers	3-1
	Particle Trajectories with Buildup of Particles	3-2
	Filter Performance for Ribbon-Like Fibers	3-4
	Mechanical Capture of Particles	3-4
IV	THE COAL USED	4-1
	Source and Preparation	4-1
	Magnetic Characterization	4-1
	Structural and Chemical Characterization	4-11
	Mössbauer Analysis	4-16
V	MAGNETIC SEPARATION OF COAL AS A WATER SLURRY	5-1
	The Separator System and Experimental Methods	5-1
	Results and Analysis	5-1
	Discussion and Conclusions	5-12
VI	MAGNETIC SEPARATION OF COAL AS A DRY POWDER	6-1
	Separator System and Experimental Methods	6-1
	Results of HGMS on Dry Coal Powders	6-2
	Conclusions and Discussions	6-5
VII	RECOMMENDATIONS	7-1
	References	7-2
Appendix A--	TYPICAL COMPUTER PROGRAM TO CALCULATE PERFORMANCE OF A HIGH GRADIENT MAGNETIC SEPARATOR	**A-1**
Appendix B--	**SUPPLEMENT TO FINAL REPORT (Period Covered: February 1 through July 15, 1977)**	**B-1**

LIST OF ILLUSTRATIONS

Figure		Page
1	Schematic Cross Section Through a Fiber Ribbon and Coordinates Used, Showing Viscous and Magnetic Forces Acting on a Particle Deposited in the nth Layer	3-2
2	Magnetization vs. Field at Room Temperature for Heavy Fraction ($\rho > 1.6$) for the -200 Mesh Size Range from a Delmont Coal Piece	4-8
3	Thermomagnetic Behavior, σ vs. T, at 10 kOe in He Atmosphere of a Heavy Fraction from -200 Mesh Sample of Delmont Coal Piece	4-10
4	Scanning Electron Micrographs and Energy Dispersive Analyses of (a) Overview of Strongly Magnetic Particles and (b) Pyrite Particle from Powdered Delmont Coal	4-12
5	Scanning Electron Micrographs and Energy Dispersive X-Ray Analysis of (a) Kaolinite Particle and (b) Calcite Particle from Powdered Delmont Coal	4-13
6	Scanning Electron Micrographs in (a) and (b) and X-Ray Maps in (c) and (d) of (b) for Fe and S, Respectively, on a Polished Surface of a Piece of Delmont Coal	4-15
7	Mössbauer Spectrum from Delmont Coal at Room Temperature	4-17
8	Mössbauer Spectrum from Fernglen Anthracite Coal at Room Temperature	4-17
9	Mössbauer Spectra of a Sieved (100 x 200) Fraction of Delmont Coal Compared to Its Light and Heavy Components Separated by Sink-Float in CCl_4	4-18
10	Mössbauer Spectra of the Feed, Mags, and Tails from the First Series of HGMS Runs: Sample #4	4-20
11	Sulfur Reduction as a Function of Field from Both Series of Runs in the HGMS Apparatus	5-4
12	Ash Reduction as a Function of Field from Both Series of Runs in the HGMS Apparatus	5-4
13	Sulfur Reductions as a Function of Velocity from Both Series of Runs in the HGMS Apparatus	5-5
14	Ash Reduction as a Function of Velocity from Both Series of Runs in the HGMS Apparatus	5-5

LIST OF ILLUSTRATIONS (Cont'd)

Figure		Page
15	Magnetic Separation Apparatus for Second Series of Tests. .	5-6
16	Sulfur and Ash in the Product as a Function of Fluid Velocity for a Variety of Applied Fields – Curves Drawn Through Data for 20 kOe; Second Series of Runs	5-8
17	Sulfur and Ash in the Product as a Function of Applied Field for a Variety of Fluid Velocities – Curves Drawn Through Data for $v \approx 2.7$ cm/s; Second Series of Runs	5-8
18	Calculated Curves and Experimental Data for Pyritic Sulfur Reduction as a Function of Field	5-10
19	Calculated Curves and Experimental Data for Pyritic Sulfur Reduction as a Function of Velocity, as Described in Figure 15 Caption.	5-10
20	Calculated Curves and Experimental Data for Ash Reduction as a Function of Field	5-11
21	Calculated Curves and Experimental Data for Ash Reduction as a Function of Velocity	5-11
22	Air System for Magnetic Separation of Dry Coal	6-1
23	Ratio of Ash Collected in Mags to Ash in Product as a Function of (Field/Velocity) for Dry Powder Separation	6-4
24	Ratio of Sulfur Collected in Mags to Sulfur in Product as a Function of (Field/Velocity) for Dry Powder Separation	6-4

LIST OF TABLES

Table		
I	Analysis of the Complete Sample.	4-2
II	Detailed Washability Analysis; Raw Delmont Coal; Size: 2 x 3/8-inch r. h.	4-2
III	Detailed Washability Analysis; Raw Delmont Coal; Size: 3/8-inch r. h. x 28 mesh	4-3
IV	Detailed Washability Analysis; Raw Delmont Coal; Size: 2-inch r. h. x 28 mesh	4-3

LIST OF TABLES (Cont'd)

Table		Page
V	Forms of Sulfur Analyses on Washability Fractions; Size: 2 x 3/8-inch r. h.	4-4
VI	Forms of Sulfur Analyses on Washability Fractions; Size: 3/8-inch r. h. x 28 mesh	4-4
VII	Froth Flotation Analysis; Raw Delmont Coal; Size: 28 mesh x 0	4-5
VIII	Feed Analysis of Coal for the Two Series of HGMS Tests	4-5
IX	Cumulative Summary of Magnetic Data on Selected Fractions from Delmont Coal	4-7
X	Ash Content After LTA from 100 x 200 Mesh Sample of Chunk No. 2 of Delmont Coal	4-11
XI	Energy Dispersive Analysis and X-Ray Diffraction Results on Selected Samples of Delmont Coal	4-14
XII	Mössbauer Analysis for Pyritic Sulfur in Feed, Mags, and Tails of HGMS Run #4 from First Series of Tests, Compared to Chemical Analysis	4-20
XIII	Mössbauer Analysis of Samples at Various Stages in Their Treatment During Sulfur Analysis	4-21
XIV	Distribution of Ash and Sulfur in First Series of Runs.	5-3
XV	Second Series of HGMS Results on Water Slurry	5-7
XVI	Input Parameters for Calculations.	5-9

Section 1

SUMMARY

A Pennsylvania coal from an upper Freeport seam has been carefully characterized physically, chemically, and magnetically. The measurements included float sink separations; ash content, total sulfur, pyritic sulfur, and sulfate sulfur as a function of size fraction; magnetic susceptibility, magnetization, and Mössbauer spectroscopy; and optical and scanning electron microscopy. High gradient magnetic separations were carried out as a function of magnetic field and fluid velocity with the powdered coal as a water slurry and as a dry air dispersion. In the water slurries both sulfur and ash were significantly reduced: 60 to 80% of the pyritic sulfur, corresponding to ~50% of the total sulfur, and ~50% of the ash were removed. In contrast to these good results, in the air dispersions the sulfur and ash reductions were much less significant: the decrease in sulfur and ash was only marginally significant. The behavior of the coal in the water slurry followed the behavior calculated from the physical models, with the magnetic properties derived from our magnetic measurements. The problem with the dry coal may be the result of local air turbulence effects, or to changes in the magnetic and physical properties of the coal. We therefore recommend further work to try to understand the difference in efficiency of separation in HGMS between water slurries and dry dispersions. We further recommend that engineering development be started on applications where HGMS can be applied to liquid slurries of coal powders – for example, in beneficiating tailings of fines from conventional coal cleaning processes, in cleaning coal for pipeline transport, or in cleaning coal dispersed in oil.

The work on this project was accomplished by Corporate Research and Development personnel of the General Electric Company (Schenectady, N.Y.) with the leadership of F.E. Luborsky; by the personnel of the Francis Bitter National Magnet Laboratory of the Massachusetts Institute of Technology (Cambridge, Mass.) with the leadership of E. Maxwell; and by personnel of the Eastern Associated Coal Corp. (Everett, Mass.) with the leadership of H.E. Harris.

Section II

INTRODUCTION

OBJECTIVE

The objective of this program was to establish the technical feasibility for removing a substantial fraction of the inorganic sulfur from dry coal powders at significant processing rates by high gradient magnetic separation (HGMS).

BACKGROUND

One of the United States' most vital current needs is an adequate supply of clean fuel. Abundant reserves of coal lie untapped because no economical means of reducing the sulfur content to acceptable levels exists. The U. S. has between 30 and 40 percent of the known world reserves of commercially producible coal, and our resources alone are estimated at 765 billion tons of economically recoverable coal. This is roughly equivalent to at least 1. 5 trillion barrels of oil, which is about 2. 5 times the current proven worldwide oil reserves. Coal is perhaps the most easily developed alternative energy source of significance available to augment costly petroleum and natural gas fuels. Among these untapped resources are large coal reserves east of the Mississippi River which have a high percentage of pyritic sulfur but are low in organic sulfur content. If sufficient pyritic sulfur were removed from these coals, they could be reclassified as low-sulfur coals.

Because of the renewed interest in coal, there is now a growing effort to create cost-effective, environmentally sound methods of utilizing coal as a clean fuel. Almost all methods for cleaning coal require grinding to a size where liberation of the sulfur-bearing phase occurs. Cleaning at the mine site is generally applicable only for larger sizes so that shipping of fine dry powders is avoided. However, for the major usage of coal (namely burning in power plants), the coal is often ground to a fine powder before burning. Thus, it is then already in a form particularly suited for physical separation techniques. However, cleaning of coal fines in a water slurry may be important in cleaning coal for pipeline transport, in cleaning coal from mine mouth wet beneficiation processes to recover the fines, or in cleaning coal in oil dispersions.

PREVIOUS WORK ON MAGNETIC DESULFURIZATION OF COAL

The first attempt to remove sulfides from finely ground coal by magnetic means appeared in a 1957 German patent[1] issued as an addition to a 1956 U. S. patent[2]; Russian work[3] in 1958 also supports the results. This early work used conventional magnets with shaped pole faces to achieve reasonable field gradients and fields for the separating force. However, pretreatments of the coal at 200° to 300°C in air or steam were used to form

films of ferromagnetic oxides on the surface of the paramagnetic sulfides to increase their magnetic susceptibility and thus enhance their removal efficiency. Studies of the same process had been reported in 1956 by Kester[4]. A low-temperature roasting in an inert atmosphere has been proposed by Fine, et al.[5] to enhance the magnetic susceptibility of the sulfur-bearing phases.

Benefaction of untreated powdered coals appeared to have been observed (Ref. 6) in 1961, confirmed[7] in 1965, and studied in more detail[8] in 1967. From 54 to 86 percent of the original pyritic sulfur was removed from four different coals. Early efforts in magnetic separation of pyrite, such as Leonard's work at West Virginia University, indicated technical feasibility; but, as he pointed out, further commercial progress awaited the development of more effective magnetic separators. In his work, four different U. S. coals were pulverized and passed through a laboratory (Franz Isodynamic) separator as dry powders. As much as 84 percent of the pyritic sulfur was removed from the Pittsburgh coal.

In contrast to these and other early efforts made with conventional magnetic circuit devices at relative low fields and trivial throughputs, recent developments in high gradient magnetic technology and in superconductivity open an entirely new dimension to the potential usefulness of magnetic separation. Trindade[9-11], working with the new high gradient magnetic separators[12, 13] developed at the Massachusetts Institute of Technology, achieved removal of approximately 90 percent of the pyritic sulfur from one Brazilian coal using water slurries. This substantial improvement over conventional processes results in part from the ability of the high gradient magnetic separation process to handle fine particles, the form of most pyritic sulfur left in coals by conventional processes. Trindade's work was extremely promising but was limited to water slurries of one type of coal and involved small-scale laboratory testing in a batch-type system. Further, for most applications dry coal is required, and the removal of the water represents a significant loss in energy. Thus, the performance of dry coal in the HGMS as well as the performance of coals from a variety of coal fields is yet to be examined. However, even for the wet slurries Trindade concluded that the HGMS process for desulfurizing coal was economically viable.

High-gradient magnetic separation results on water slurries of other coals have recently been reported. Murray[14] used coals from Warrick County, Indiana, containing over 4% total sulfur, about half organic and half inorganic. For the coal ground to 99% below 74 μm (200 mesh) using a stainless steel roving packed in the canister, for 20 kOe applied field, he obtained reductions of inorganic sulfur in two different samples of 55% and 78% for 120 s retention time in the filter. Three passes through the filter at 30 s retention time increased the removal of inorganic sulfur to 67% and 85%.

Lin et al.[15] also reported results for high gradient separation of water slurries of coal. The coal used was an Illinois coal with 1.17% pyritic sulfur, 0.03% sulfate sulfur, and 1.90% organic sulfur for a total of 3.10%. This was

ground to a mean particle size of 33 μm; 99% less than 65 μm. A variety of experimental variables was used. For a stainless steel packing, using 20 kOe, 28.4% of the total sulfur was removed. This would correspond to 75% removal of the pyritic sulfur. At the same time 45.6% of the ash minerals were removed.

An open field annular quadrupole magnet inside a corresponding slurry channel has been used[16] on two Pennsylvania coals with very high pyritic contents. This type of separator works by the development of a secondary circulation transverse to the primary orbital circulation, which brings the particles closer into the region of high field intensity. One of the coals yielded 81% recovery of cleaned coal with 83% removal of pyritic sulfur.

The only high gradient separation of dry coal powders was reported in 1976 by Murray[14] in the same work on water slurries described above. Stainless steel screens were used in the canisters. After three passes of dry coal through the filter, for the two different Indiana coals only 25% and 39% of the inorganic sulfur was removed, in contrast to the 67% and 85% removed when in the water slurry. There was no indication in the paper as to why the removal of pyrite was less efficient for the dry powders.

These recent developments in the magnetic separation technology applied to cleaning coal have been summarized in two recent papers by Liu and Lin[17] and by Oder[18]. These have all been published since the work on the contract started. This new work on cleaning water slurries of coal thoroughly confirms the original publications of Trindade (based only on work using a Brazilian coal). The one publication which has now appeared and is concerned with cleaning dry coal powders in a high gradient separator has confirmed our suspicion that it will not be as efficient as cleaning of water slurries but provides no answers as to why.

Section III

MAGNETIC SEPARATOR MODELING THEORY

The basic incentive of the modeling is the need to develop the conceptual understanding, as well as the quantitative models, necessary to predict the technical performance of a particular system so that the economics can be predicted without extensive trial-and-error testing. In the next sections we will outline the model.

The problem is to calculate the motion of a paramagnetic particle traveling in a fluid stream in the presence of a magnetized fiber. First calculations[19, 20] assumed a fiber with circular cross section, with its long axis perpendicular to the field and velocity vectors, and magnetized uniformly to saturation. These analyses followed the analogous analysis[21] carried out for electrostatic filters. In order to arrive at an exact solution to the equations of motion, only the magnetic and drag forces were considered. Simplifying assumptions were made by neglecting fluid boundary layer changes around the fiber. For the fluid flow, two cases were considered: (1) for high Reynolds numbers where the inertial forces are much greater than the frictional forces, the potential flow equation is valid, and (2) for Reynolds number $<<1$ where the inertial forces are included in an approximate way.

THEORETICAL ANALYSIS

Calculations for Ribbon-Like Fibers

A model approximating the conditions used to obtain the experimental results on CuO/Al_2O_3 particles[22, 23] was next developed. A steel wool fiber packing was used in the filter; thus the filter performance was calculated assuming an infinite ribbon instead of a rod. However, as a first approximation we assumed that the field and flow lines on the upstream side of the fiber are the same as for the circular cylinder previously calculated (Refs. 24-26).

Let us now compare the weight of CuO particles actually captured in the filter, ~5 to 85 gms, compared to the maximum weight W_m that can be held on the first monolayer in the active area. The active area is the area of the one upstream edge of the fiber where particles are captured. From geometric considerations based on Figure 1, assuming only 1/3 of the fibers are now correctly oriented,

$$W_m = \pi f P W \rho_p (T + 2P)/9ST\rho_f \qquad (1)$$

where W = total weight of fibers in the filter, ρ_p and ρ_f are the densities of the particles and fibers, and f is the fraction of the fibers which are active

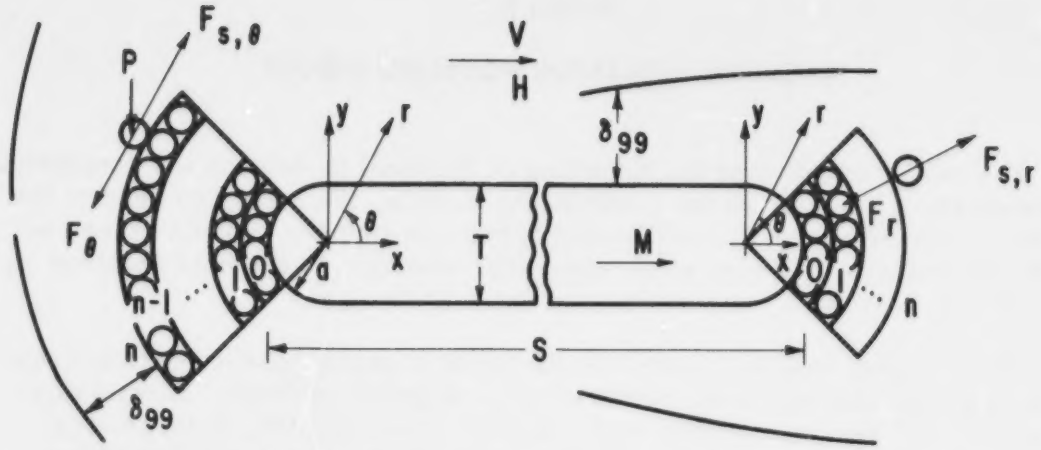

Figure 1. Schematic Cross Section Through a Fiber Ribbon and Coordinates Used, Showing Viscous and Magnetic Forces Acting on a Particle Deposited in the nth Layer

in capturing particles, i.e., the capture efficiency. Using the values given (Refs. 22, 23), $W_m = 0.52$ gms for the first layer. Thus, it is apparent that many layers of particles must build up on the fibers. We consider here only the case for large V_m/V, where the buildup fans out as approximated in Figure 1.[27, 28] Thus, it is readily shown that each layer η will hold increasing weights

$$W_{m,n} = \pi f P W \rho_p [T + 2P(1 + 2n)]/9ST\rho_f. \quad (2)$$

Particle Trajectories with Buildup of Particles

The fluid flow sees a changing radius as the particle layers build up, given by

$$a_n = a + 2Pn. \quad (3)$$

Assuming potential flow as before, the flow potential is

$$\Psi(\text{flow}) = Vr\cos\theta + (Va_n^2/r)\cos\theta. \quad (4)$$

The field potential is assumed to be unaffected by the buildup of particles, i.e., the permeability of the particles is assumed to be near that of the fluid. Then

$$\Psi(\text{field}) = -rH\cos\theta + [(\mu - 1)Ha^2/(\mu + 1)r]\cos\theta \quad (5)$$

where μ = permeability of the fiber.

The fluid velocity components are then

$$\left.\begin{aligned} V_r &= \delta \Psi/\delta r = V\cos\theta - (Va_n^2/r^2)\cos\theta \\ V_\theta &= \delta \Psi/r\delta\theta = -V\sin\theta - (Va_n^2/r^2)\sin\theta \end{aligned}\right\} \tag{6}$$

and the field components

$$\left.\begin{aligned} H_r &= H\cos\theta + [(\mu - 1)Ha^2/(\mu + 1)r^2]\cos\theta \\ H_\theta &= -H\sin\theta + [(\mu - 1)Ha^2/(\mu + 1)r^2]\sin\theta \end{aligned}\right\} . \tag{7}$$

Since the experimental data for CuO covers fields from 5 kOe to 100 kOe and fields $> 2\pi M_S = 7500$ Oe are required to saturate a cylindrical rod across its diameter, we consider two regions. For $H > 7500$ Oe, the fiber is assumed saturated. Then

$$(\mu - 1)/(\mu + 1) = 2\pi M_S/H \tag{8}$$

for $H < 7500$ Oe we assume that $\mu \gg 1$ and then

$$(\mu - 1)/(\mu + 1) = 1. \tag{9}$$

The force on the particles

$$F = (4\pi P^3/3)\,\nabla\,(M \cdot H)/2 \tag{10}$$

for saturating fields is evaluated to be

$$\left.\begin{aligned} F_r &= (16\pi^2\chi M_S P^3 a^2/3r^3)[(2\pi Ma^2/r^2) + H\cos 2\theta] \\ F_\theta &= -(16\pi^2\chi M_S P^3 a^2/3r^3)\sin 2\theta. \end{aligned}\right\} \tag{11}$$

The differential equations of motion for this system

$$\left.\begin{aligned} dr/dt &= F_r/6\pi\eta P + V_r \\ rd\theta/dt &= F_\theta/6\pi\eta P + V_\theta \end{aligned}\right\} \tag{12}$$

become

$$\frac{dr_a}{r_a d\theta} = \frac{[1 - (a_n/ar_a)^2]\cos\theta - (V_m/Vr_a^3)[(2\pi M_S/Hr_a^3) + \cos 2\theta]}{[1 + (a_n/ar_a)^2]\sin\theta + (V_m/Vr_a^3)\sin 2\theta.} \tag{13}$$

As for the case when $n = 0$, i.e., $a_n/a = 1$, this equation has an analytic solution only when $2\pi M_S/H = 0$; namely

$$y_a^{\infty} = r_a[1 - (a_n/ar_a)^2] \sin\theta - (V_m/2Vr_a^2) \sin 2\theta. \quad (14)$$

The critical entering coordinate is now

$$\left.\begin{aligned} \zeta &= (V_m/2V)\,(a/a_n)^2, \quad \text{if } (V_m/V) \le 2^{1/2}\,(a_n/a)^2 \\ &= (\text{constant})_{\text{sing}}, \quad \text{if } (V_m/V > 2^{1/2}\,(a_n/a)^2 \end{aligned}\right\}. \quad (15)$$

Some typical trajectories and the dependence of ζ on V_m/V are shown by Luborsky(29) for various values of n. For smaller values of H, for example when $H = 2\pi M_S$, the complete equation (13) has been solved by numerical integration, using the 4th order Runge-Kutta approximation. Only the exact solution approximation is used in most of the calculations. With this approximation, ζ for an unsaturated fiber is also given by (15) but with V_m replaced by $V_{m,u}$ where

$$V_{m,u} = 4\chi P^2 H^2/9\eta a. \quad (16)$$

Filter Performance for Ribbon-Like Fibers

We have assumed that, on-average, only 1/2 as many ribbon-like fibers are correctly oriented to interact with the particles in the stream as was the case for cylindrical fibers. The fractional recovery of magnetic particles is now

$$R = 1 - \exp(-fFL\zeta/3S). \quad (17)$$

MECHANICAL CAPTURE OF PARTICLES

Because of the very irregular nature of the packing of the steel wool fibers in the filter, we expect a significant fraction of the particles to be mechanically trapped. This has been found(30) to be true in electrostatic filters. We therefore write, for the total fractional recovery of paramagnetic particles

$$R = 1 - \exp[-fFL(\zeta + \xi)/3S] \quad (18)$$

where 2ξ is a reduced cross section for mechanical capture.

The mechanical recovery fraction is

$$R_m = 1 - \exp[-fFL\xi/3S]. \quad (19)$$

We have found no means of calculating ξ from first principles. Instead we say, a priori, that ξ should be proportional to S + 2P, and proportional to 1/V as suggested by the experimental data. The 1/V dependence is expected from the increasing kinetic energy of the particle, which will prevent sticking or will knock off particles previously deposited. Thus

$$\xi = Q' (S + 2P)/2Va \tag{20}$$

where Q' is a proportionality factor to be adjusted to fit for the entire filter.

The purity, or "grade" G, of the captured material can now be calculated by assuming that the paramagnetic and diamagnetic particles are mechanically captured with equal efficiency and that no other factors affecting purity, such as agglomeration between Al_2O_3 and CuO particles, are significant. Then

$$G = Rw_p/(Rw_p + R_m w_d) \tag{21}$$

where w_p = weight of paramagnetic and w_d = weight of diamagnetic particles entering. We next consider, in an approximate way, the effect of the boundary layer, following the procedure of Luborsky.[31] For impingement of a fluid on the front of a circular cylinder, the boundary layer thickness, δ_{99}, averaged over the region of interest: i.e., from 135° to 180°, is given approximately[32] by

$$\delta_{99} = \pi^{1/2} (\eta a_n/V\rho)^{1/2} \tag{22}$$

where η and ρ are the fluid viscosity and density, respectively. This gives a minimum value of $\delta_{99} = 0.0018$ cm for n = 0, and larger values as n increases, for the maximum velocity of 20 cm/s used in the CuO-Al_2O_3 experimental work. Since the particle diameter of the CuO, 2P, is smaller than δ_{99}, we use an entrance velocity, V, reduced by P/δ_{99} as the velocity impinging on the particle. Thus

$$F_{s,\theta} = 6P^2 (\pi\eta V^3\rho/a_n)^{1/2} [1 + (a_n^2/r^2)] \sin\theta \ . \tag{23}$$

As the layers buildup, the radial coordinate of the particles is assumed to increase in steps given by

$$r = a + (2n + 1) P \tag{24}$$

Setting Equation 11 for F_θ equal to Equation 23, we can solve for the critical angle θ_c for each layer of particles on the fiber structure. All particles in the region of angles greater than θ_c are thus swept off. From geometric considerations the mass of particles removed from each layer per unit length of fiber is then:

$$W_r' = (\pi - 4\theta_c) [2 (1 + 2n) P + T] P\rho_p/2 \tag{25}$$

where ρ_p is the particle density. Applying the previously described corrections, the weight of particles removed in each segment of the filter, ℓ, is

$$W_r = (\pi - 4\theta_c) [2(1 + 2n) P + T] P\rho_p W\ell f/9\rho_f STL \tag{26}$$

where we consider that only a fraction, f, of the fibers are active, only 1/3 are correctly oriented for capture, the packing fraction of particles in the layer is 2/3, and W is the total weight of fibers, having a density of ρ_f in the total filter length, L.

In the previous calculation[29] the recovery of particles on the downstream edge of the fibers was not considered. This capture on the downstream edge is observed experimentally[27, 28, 33, 34] but cannot be accounted for by tracing particle trajectories. We suggest that the particles arrive by being swept off the front edge or by being caught up in the turbulent wake of the fiber. Without defining the mechanism of arrival we now consider capture on the downstream edge by assuming that capture of particles occurs with the same geometry as on the upstream edge. We then apply criteria similar to those used on the upstream edge to determine the fraction of the particles remaining and their configuration. On the downstream edge the critical angle occurs when the radial component of the magnetic force, F_r, is equal to the radial component of the shear force, $F_{s,r}$, where

$$F_r = (16\pi^2 P^3 \chi M_s a^2/3r^3)[(2\pi M_s a^2/r^2) + H\cos 2\theta] \tag{27}$$

and

$$F_{s,r} = 6\pi\eta P V_r = 6\pi\eta P\,[1 - (a_n^2/r^2)]\,V\cos\theta. \tag{28}$$

In this case the boundary layer thickness is taken as equivalent to that at the end of a flat plate, namely

$$\delta_{99} = 5(\eta S_n/V\rho)^{1/2} \tag{29}$$

where S_n, the width of the ribbon, is a function of n given as $S_n \approx S + 2nP$. Substituting

$$F_{s,r} = 1.2\pi P^2\,(\eta V^3\rho/S_n)^{1/2}\,[1 - (a_n^2/r^2)]\cos\theta. \tag{30}$$

Equating Equation 27 with 30 and solving for θ gives the critical angle for particles on each layer of the downstream edge of the fiber. The weight of particles swept off is calculated from Equation 26 again.

The recovery and purity of the material captured in each element of the filter is calculated as described previously, but the weight, W_r, is returned to the stream to enter the next filter element together with the other particles in the stream. A typical computer program to carry out these calculations is listed in Appendix **A.**

The theoretical analysis developed above works well for separations in liquids at reasonably low Reynolds numbers. However, in gas streams inertial forces on the particle should be considered. This has been discussed

in some detail, for example by Lawson.[35] In addition, more complicated fluid flow will probably exist, which will strongly affect capture efficiency and the geometry of the buildup of the particles. These effects have not yet been incorporated into the modeling equations.

Section IV

THE COAL USED

SOURCE AND PREPARATION

The source of the coal to be used was decided on with the concurrence of Dr. W. Spackman and Mr. Deurbrouck. It came from an Upper Freeport seam in Westmoreland County, PA: the Delmont mine. An original sample was rejected because of excessive roof clay. A more representative sample of about 3000 lbs labeled Delmont # 7945 was packed in drums for transit.

Prior to any processing, large pieces of rock were removed by hand, a treatment that simulates commercial plant preparation, in which rock material would be removed by a Bradford breaker before the raw coal was fed to the preparation plant. The coal sample was screened at 2 inches and the +2-inch material was crushed to minus 2 inches and then recombined with the original minus 2-inch material. This sample was then thoroughly mixed and a subsample of about 1200 lbs was obtained from the larger sample. This 1200 lb sample was subsequently subdivided into 6 samples, each containing about 200 lbs. One of these samples was air dried and sized; wet screening was used for material less than 100 mesh. The size analysis is shown in Table I. Ash and the forms of sulfur and their percentages for the various size fractions are also given in Table I.

Float-sink separations were carried out and ash, total sulfur, and forms of sulfur were made on the various size and specific gravity fractions. The distribution of ash and total sulfur in the float-sink separations are given in Tables II and III for two different size ranges and in Table IV for the combined range of sizes, representing 88.1% of the total sample. The percentages of the three forms of sulfur (pyritic, sulfate, and organic) in the float-sink fractions are given in Tables V and VI for the same two size ranges reported in Tables II and III. Froth flotation tests were run on the 28 mesh x 0 size. All analyses, except forms of sulfur, were run on the froth increments. These results are shown in Table VII. Two independent series of separation experiments were carried out with this coal but with different size fractions. The analyses of this feed coal for the two series are shown in Table VIII. In the first series a 48x100 mesh fraction was used, but in the second series the entire coal was ground to -60 mesh.

MAGNETIC CHARACTERIZATION

Magnetic susceptibility measurements were carried out on various samples of the Delmont coal supplied by EAC, using a vibrating sample

Table I

ANALYSIS OF THE COMPLETE SAMPLE

Size	DISTRIBUTION		FORMS OF SULFUR ANALYSES ASTM Designation 2492-68				ASH
	Weight Percent	Cum. Weight Percent	Total Sulfur Percent	Pyritic Sulfur Percent	Sulfate Sulfur Percent	Organic Sulfur Percent	Percent
2 x 1 1/2-in. r.h.	2.2	2.2	2.84	2.48		0.36	27.8
1 1/2 x 1 -in. r.h.	5.5	7.7	1.84	1.37		0.47	38.8
1 x 3/4 -in. r.h.	5.6	13.3	1.89	1.50		0.39	39.0
3/4 x 1/2 -in. r.h.	10.1	23.4	1.64	1.26		0.38	26.9
1/2 x 3/8 -in. r.h.	6.4	29.8	1.58	0.97		0.61	18.8
3/8 x 1/4 -in. r.h.	15.3	45.1	1.54	1.07		0.47	15.2
1/4 x 1/8 -in. r.h.	19.9	65.0	1.51	1.04		0.47	12.6
1/8 in. r.h. x 14 mesh	13.2	78.2	1.77	1.12		0.65	10.7
14 x 28 mesh	9.9	88.1	1.54	1.10		0.44	10.1
28 x 48 mesh	3.4	91.5	1.73	1.00		0.73	10.3
48 x 100 mesh	3.8	95.3	2.23	1.25		0.98	10.8
100 x 200 mesh	1.8	97.1	2.10	0.87		1.23	11.2
200 x 325 mesh	0.6	97.7	1.63	0.88		0.73	11.8
minus 325 mesh	2.3	100.	1.03	0.51		0.52	16.7

Negligible

Table II

DETAILED WASHABILITY ANALYSIS

Raw Delmont Coal

Size: 2 x 3/8-inch r. h.

(29.8 percent of total)

Sink	Float	Weight %	Ash %	Sulfur %	CUMULATIVE FLOAT Weight %	CUMULATIVE FLOAT Ash %	CUMULATIVE FLOAT Sulfur %	CUMULATIVE SINK Weight %	CUMULATIVE SINK Ash %	CUMULATIVE SINK Sulfur %
	1.30	41.2	3.6	0.90	41.2	3.6	0.90	100.0	25.2	2.02
1.30	1.35	13.5	8.5	1.38	54.7	4.8	1.02	58.8	40.3	2.82
1.35	1.40	3.8	12.8	2.80	58.5	5.3	1.13	45.3	49.8	3.23
1.40	1.45	2.4	16.6	4.21	60.9	5.8	1.25	41.5	53.2	3.27
1.45	1.50	1.5	20.7	2.74	62.4	6.1	1.29	39.1	55.5	3.21
1.50	1.55	2.1	20.9	2.88	64.5	6.6	1.34	37.6	56.8	3.23
1.55	1.60	2.6	25.9	3.21	67.1	7.4	1.42	35.5	59.0	3.25
1.60	-	32.9	61.6	3.25	100.0	25.2	2.02	32.9	61.6	3.25

Table III

DETAILED WASHABILITY ANALYSIS
Raw Delmont Coal
Size: 3/8-inch r. h. x 28 mesh
(58.3 percent of total)

Sink	Float	Weight %	Ash %	Sulfur %	CUMULATIVE FLOAT Weight %	CUMULATIVE FLOAT Ash %	CUMULATIVE FLOAT Sulfur %	CUMULATIVE SINK Weight %	CUMULATIVE SINK Ash %	CUMULATIVE SINK Sulfur %
-	1.30	66.0	2.6	0.69	66.0	2.6	0.69	100.0	13.5	1.55
1.30	1.35	12.8	7.6	1.22	78.8	3.4	0.78	34.0	34.8	3.21
1.35	1.40	3.0	13.0	2.46	81.8	3.8	0.84	21.2	51.2	4.42
1.40	1.45	1.2	16.7	2.97	83.0	4.0	0.87	18.2	57.4	4.74
1.45	1.50	0.9	20.6	3.24	83.9	4.1	0.89	17.0	60.3	4.86
1.50	1.55	0.7	23.5	3.30	84.6	4.3	0.91	16.1	62.6	4.96
1.55	1.60	0.9	31.0	3.68	85.5	4.6	0.94	15.4	64.3	5.03
1.60	-	14.5	66.4	5.12	100.0	13.5	1.55	14.5	66.4	5.12

Table IV

DETAILED WASHABILITY ANALYSIS
Raw Delmont Coal
Size: 2-inch r. h. x 28 mesh
(88.1 percent of total)

Sink	Float	Weight %	Ash %	Sulfur %	CUMULATIVE FLOAT Weight %	CUMULATIVE FLOAT Ash %	CUMULATIVE FLOAT Sulfur %	CUMULATIVE SINK Weight %	CUMULATIVE SINK Ash %	CUMULATIVE SINK Sulfur %
-	1.30	57.6	2.9	0.76	57.6	2.9	0.76	100.0	17.7	1.79
1.30	1.35	13.1	7.9	1.28	70.7	3.8	0.86	42.4	37.9	31.9
1.35	1.40	3.3	12.9	2.58	74.0	4.2	0.93	29.3	51.3	4.04
1.40	1.45	1.6	16.7	3.05	75.6	4.5	0.98	26.0	56.2	4.22
1.45	1.50	1.0	20.6	2.90	76.6	4.7	1.00	24.4	58.7	4.30
1.50	1.55	1.2	22.7	3.15	77.8	5.0	1.04	23.4	60.4	4.36
1.55	1.60	1.5	29.3	3.52	79.3	5.4	1.08	22.2	62.4	4.42
1.60	-	20.7	64.8	4.49	100.0	17.7	1.79	20.7	64.8	4.49

Table V

FORMS OF SULFUR ANALYSES ON WASHABILITY FRACTIONS
Size: 2 x 3/8-inch r. h.
(29. 8 percent of total)

Sink	Float	Weight %	Ash %	Total Sulfur, %	Pyritic Sulfur, %	Sulfate Sulfur, %	Organic Sulfur, %
----	1.30	41.2	3.6	0.90	0.54	↑	0.36
1.30	1.35	13.5	8.5	1.38	1.02		0.36
1.35	1.40	3.8	12.8	2.80	2.29		0.51
1.40	1.45	2.4	16.6	4.21	3.68	Negligible	0.53
1.45	1.50	1.5	20.7	2.74	2.39		0.35
1.50	1.55	2.1	20.9	2.88	2.76		0.12
1.55	1.60	2.6	25.9	3.21	2.82		0.39
1.60	----	32.9	61.6	3.25	3.21	↓	0.04

Table VI

FORMS OF SULFUR ANALYSES ON WASHABILITY FRACTIONS
Size: 3/8-inch r. h. x 28 mesh
(58. 3 percent of total)

Sink	Float	Weight %	Ash %	Total Sulfur, %	Pyritic Sulfur, %	Sulfate Sulfur, %	Organic Sulfur, %
----	1.30	66.0	2.6	0.69	0.23	↑	0.46
1.30	1.35	12.8	7.6	1.22	0.86		0.36
1.35	1.40	3.0	13.0	2.46	1.80		0.66
1.40	1.45	1.2	16.7	2.97	2.75	Negligible	0.22
1.45	1.50	0.9	20.6	3.24	2.87		0.37
1.50	1.55	0.7	23.5	3.30	2.93		0.37
1.55	1.60	0.9	31.0	3.68	3.66		0.02
1.60	----	14.5	66.4	5.12	5.67*	↓	----

*This value is doubtful

Table VII

FROTH FLOTATION ANALYSIS
Raw Delmont Coal
Size: 28 mesh x 0
(11.9 percent of total)

Increment	Weight %	Ash %	Sulfur %	Cumulative Weight %	Cumulative Ash %	Cumulative Sulfur %
1	31.9	3.1	0.98	31.9	3.1	0.98
2	42.8	4.8	1.21	74.7	4.1	1.11
3	13.0	11.5	1.94	87.7	5.2	1.24
4	4.1	28.5	3.14	91.8	6.2	1.32
5	3.1	41.6	4.16	94.8	7.4	1.41
6	2.4	57.3	5.35	97.3	8.6	1.51
Tailings	2.7	75.5	5.79	100.0	10.4	1.62

Time release method with MIBC

Table VIII

FEED ANALYSIS OF COAL FOR THE
TWO SERIES OF HGMS TESTS

	FIRST SERIES		SECOND SERIES
Moisture	0.6 to 0.8%		
Ash	12.6%		16.9%
Total S	1.84		1.58
Pyritic S	0.94		1.30
Organic S	0.90		0.28
Size distribution	48 x 100	44.7%	60 x 0
	100 x 200	21.2	
	200 x 325	7.1	
	-325	27.0	

magnetometer (VSM) of the Foner design (PAR Model FM-1) at room temperature and at lower temperatures in a liquid helium dewar, in fields ranging from -20 kOe to +20 kOe. For a few samples, thermomagnetic characterization, i.e., magnetization at fixed field vs temperature, up to 600°C in a helium atmosphere was carried out.

As received, a cylindrical chunk of Delmont coal was found to be diamagnetic at room temperature with $\chi_g = -0.6 \pm 0.1 \times 10^{-6}$ emu/g-Oe and with no discernible ferromagnetic component of magnetization. A sample from the same piece (originally ~3 in. cube) was ground in a porcelain mortar and pestle. No sieving or powder classification was made. The powdered coal also showed a diamagnetic susceptibility of about the same value. These results agree with literature values.

In order to focus on the inorganic minerals presumed to carry sulfur and iron, a one-step float-sink separation was effected. Coal was hand ground and sieved with Tyler sieves. The fractions between mesh sizes (-32, +100), (500 μm to 250 μm), (-100, +200), (75 μm to 150 μm), and -200 (less than 75 μm) were separately collected and processed through a pear-shaped separatory funnel with CCl_4. The density of CCl_4 is $\rho \approx 1.6$, so that coal ($\rho \approx 1.25$-1.3) will float, and most pyritic minerals and ash materials will sink if liberated. About 2% of the (-100, +200) and -200 fractions sank, while about 5% of the (-32, +100) fraction sank. Initial magnetic measurements on the heavy fractions of the two larger sized powders yielded paramagnetic susceptibilities at room temperature, with values $\chi_g = +2.4 \pm 0.1 \times 10^{-6}$ emu/g-Oe and $+2.7 \pm 0.1 \times 10^{-6}$ emu/g-Oe, respectively, but again with no discernible ferromagnetic component. (Table IX; samples 1-V3H and 1-V3HA.

Low temperature measurements of the heavy fraction of (-100, +200) material showed the presence of a nearly Curie-law component. At 30K the susceptibility had increased by a factor of seven to $\chi_g = 17.7 \times 10^{-6}$ emu/g-Oe (valid to 20 kOe) with negligible ferromagnetic component. A rough preliminary analysis of data between 6K and 70K, plus the 300K point permits a description in terms of a Curie-Weiss behavior and a temperature independent term (including diamagnetism), i.e.

$$\chi_g = \chi_{c\text{-}w} + \chi_{TIP} \tag{31}$$

$$= \frac{C}{T-\theta} + \chi_{TIP} \tag{32}$$

Roughly $\theta = -5$ to -10K and $\chi_{TIP} \approx 0 \rightarrow 2.3 \times 10^{-6}$ emu/g-Oe. Treating $C = N_{cw} g^2 \beta^2 S(S+1)$ as applicable to Fe^{2+} ions ($S = 2$, $g \approx 2.1$ to 2.2), we find $N_{cw} \approx 1 \times 10^{20}$ Fe^{2+} ions/gram of heavy fraction. This N_{cw} is not total iron but is only that portion exhibiting a localized spin magnetic behavior (Curie-Weiss behavior) in the as-received state. This result may be compared to observations on all significant iron species as seen in the Mössbauer spectrometer.

Table IX

CUMULATIVE SUMMARY OF MAGNETIC DATA ON SELECTED FRACTIONS FROM DELMONT COAL[a]

Sample	Size (mesh)	Wt Fraction[b]	σ_0(R.T.) emu/g	χ_g(R.T.) emu/g-Oe	Remarks
1-V3H[c]	32x100	0.05	~0	2.7×10^{-6}	
1-V3HA	100x200	0.02	~0?	2.4×10^{-6}	"Curie-law" χ (40K)=6χ(295K)
1-V4H[d]	100x200	--	0.009	2.56×10^{-6}	Frantz Separator moderately magnetic fraction
1-V5H	-200	0.02	0.058	2.54×10^{-6}	Same Curie-law ratio
2-V2H[e]	100x200	0.05	0.024	1.6×10^{-6}	Same Curie-law ratio
2-V3H	-200	--	0.015	1.2×10^{-6}	
MIT Run #4 Mags, 64kG	-48		~0.012	0? ~$.4\times10^{-6}$?	σ_0(40K)≈0.012; χ_g(40K)≈7.7×10^{-6}
Light fraction fresh grind	100x200	--	~0	<0	
aged 8 wks			0.13	~0	In room air during June/July
Fresh grind + 15 hrs in H_2O	-200	entire sample	0.022	~0	Distilled water, pH=7.4
2-post LTA:	100x200				
heavy fraction		--	0.017 (0.013)[g]	2.0×10^{-6}	+ Curie-law[f]
whole coal		--	0.045 (0.003)[g]	3.5×10^{-6}	+ Curie-law
light fraction		--	0.118 (0.004)[g]	5.4×10^{-6}	

a) Samples designated 1-xxx, 2-xxx, ··are from individual chunks.
b) Fraction of heavy to total material of this size cut.
c) Reported previously; H=heavy = sinks in CCl_4.
d) Frantz Isodynamic Separator runs. Field current settings, I_H=1.0 and 1.5 A. Strongest magnetic fraction (0.5 amp) previously removed.
e) Subjected to LTA and remeasured.
f) Sampling problem: average σ_0 from two runs with σ_0=0.023, 0.010.
g) Calculated as per gram of material before LTA.

For further identification/characterization the heavy fraction of (-100, +200) was passed through the Frantz Isodynamic Separator (forward slope 30°, side slope +10°) at field current strengths of 0.5, 1.0, and 1.5 A. The magnetic fractions have considerably more translucent or transparent crystals (~50%) when viewed at 60X than the "nonmagnetic" fraction (~10%). The major components of the "nonmagnetic" heavy mineral fraction are FeS_2, kaolinite, and $CaCO_3$, as found by X-rays. The major X-ray-determined components of the magnetic fraction appear to be calcite-siderite intermediate compositions [(Ca; Fe)CO_3]. Further aspects of chemical and structural analyses are given in the next section.

Additional magnetization measurements were made on other liberated mineral fractions (heavy mineral particles which sink in CCl_4) for various size classifications, after beneficiation in the Frantz laboratory magnetic separator, and on a sample of the "mags" from a preliminary water slurry HGMS run. Several of these same samples, along with their associated materials, e.g., feed, tails, light fractions, etc., were also examined by SEM (Scanning Electron Microscopy), energy dispersive analysis, and Mössbauer spectroscopy, as reported in the next sections.

The magnetization measurements are summarized in Table IX. The curves, such as those shown in Figure 2, of total magnetization per gram, σ, are decomposed for $H \gtrsim 5$ kOe, so that $\sigma = \sigma_0 + \chi_g H$. Among notable features is the reproducible "Curie-law" behavior. From X-ray, SEM data, and Mössbauer spectra, we shall associate this partly with a siderite-calcite component and partly with iron in a clay-like component of the mineral matter. The variability from sample to sample is illustrated by the changes between samples from chunks #1 and #2 (e.g., 1-xxx, 2-yyy). Whereas, in the (100 x 200) size fraction it took magnetic separation to bring out a small spontaneous magnetization component, σ_0, in the heavy fraction from chunk #1, this appeared readily without magnetic separation in chunk #2 (compare samples 1-V3HA, 1-V4H, 2-V2H). Another aspect of the variability relating to the extent of liberation is the very marked increase in σ_0 on going to -200 mesh (heavy) material in the case of chunk #1 (1-V5H), which may be contrasted with the lack of increase for chunk #2 (2-V3H vs. 2-V2H).

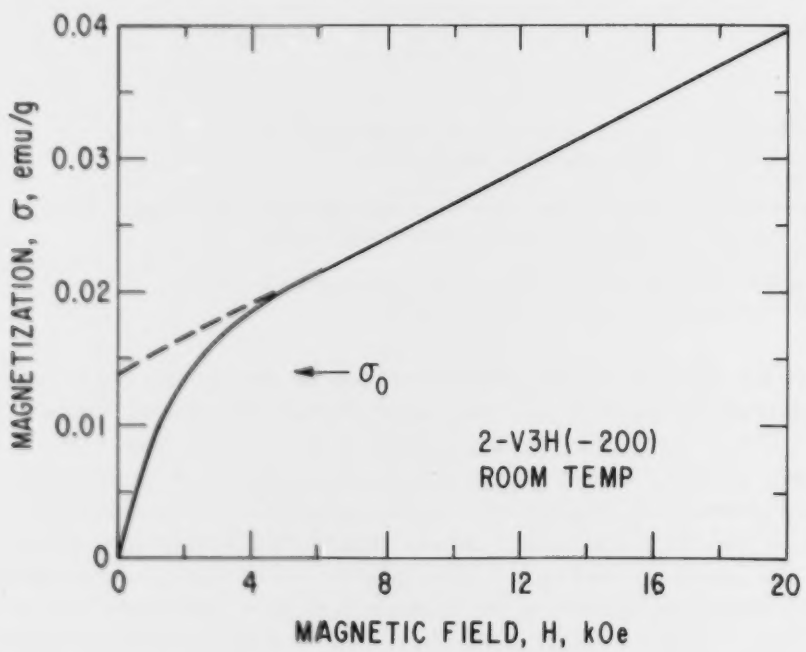

Figure 2. Magnetization vs. Field at Room Temperature for Heavy Fraction ($\rho > 1.6$) for the -200 Mesh Size Range from a Delmont Coal Piece

Size distribution of pyrite is obviously all-important for liberation. SEM studies on Iowa coals by Professor R. T. Greer of Iowa State University show very important concentrations of pyrites at very small size: e.g., below 10 μm, in contrast to optical microscopy. In Delmont coal we have not seen such small pyrite particles. It may be argued that χ_g does not change much with the mineral fraction particle sizes herein, and that the contribution to total magnetization at 20 kOe and above comes mostly from the $\chi_g H$ term of $\sigma = \sigma_0 + \chi_g H$. (In other words, σ_0 is not really important.) However, the Curie-law behavior of χ_g and our proposed attribution of this to siderite-calcite minerals and iron-bearing clays leaves us uncertain as to the relevance of these arguments to the desulfurization goal.

With regard to the data from the HGMS test sample (MIT, Run #4, mags) it may be of interest that σ_0 has roughly the same value as found in the heavy fractions of sample #2 and the laboratory-magnetically separated #1-V4H. If the same Curie-law behavior held for this MIT mags sample, we should have found χ_g (R. T.) $\approx 1.3 \times 10^{-6}$ emu/g-Oe. The rather less certain and lower value we report is either a real effect or a manifestation of experimental difficulties. Interesting results on this sample from Mössbauer spectrometry are given in the next section.

Another category of result of significance concerns the changes in coal by handling. A light fraction of Delmont No. 2 (100 x 200) was aged in room air for the humid eight weeks of June and July. It developed a spontaneous moment, σ_0 (R. T.) = 0.13 emu/g (i.e., per gram of light fraction!), with no measureable χ_g (R. T.). If this value were to be referred to the LTA ash residue, it would be 30x higher (i.e., σ_0 = 3.5 emu/g!). An effort is made below to identify what has happened. Freshly ground light fraction is diamagnetic.

In a related (and controlled) experiment, freshly ground whole coal (-200) was aged 15 hours in distilled water with a pinch of Alconox, so that the resulting slurry had a pH of 7.4. The sample developed a spontaneous magnetization $\sigma_0 = 0.022$ emu/g with $\chi_g \approx 0$. This finding could be rather important for interpretation of HGMS data.

The presence of spontaneous magnetization (σ_0) components in the various samples described above is a continuing curiousity as well as a tantalizing fact of potential importance for the magnetic separation process. The "curiosity" arises because spontaneous magnetization is not a property of any of the dominant minerals identified in the coal fractions studied. In Figure 3 we show a thermomagnetic curve, σ vs T, at a constant field, H, of 10 kOe for sample 1-V5H (-200), a heavy mineral fraction selected because of its high value for σ_0 (R. T.). The sample magnetization σ (10 kOe, T) was recorded continuously during heating in a helium gas atmosphere to 600°C and back. About half of the magnetization is associated with a Curie point near 300°C, a temperature highly suggestive of the presence of a ferrimagnetic pyrrhotite (Fe_xS, where x is slightly less than unity). Its magnitude is very small, being about one or two percent of the estimated pyrite, which, in turn, is about one to two percent of the coal. Thus, the (presumed) pyrrhotite escapes detection in other methods.

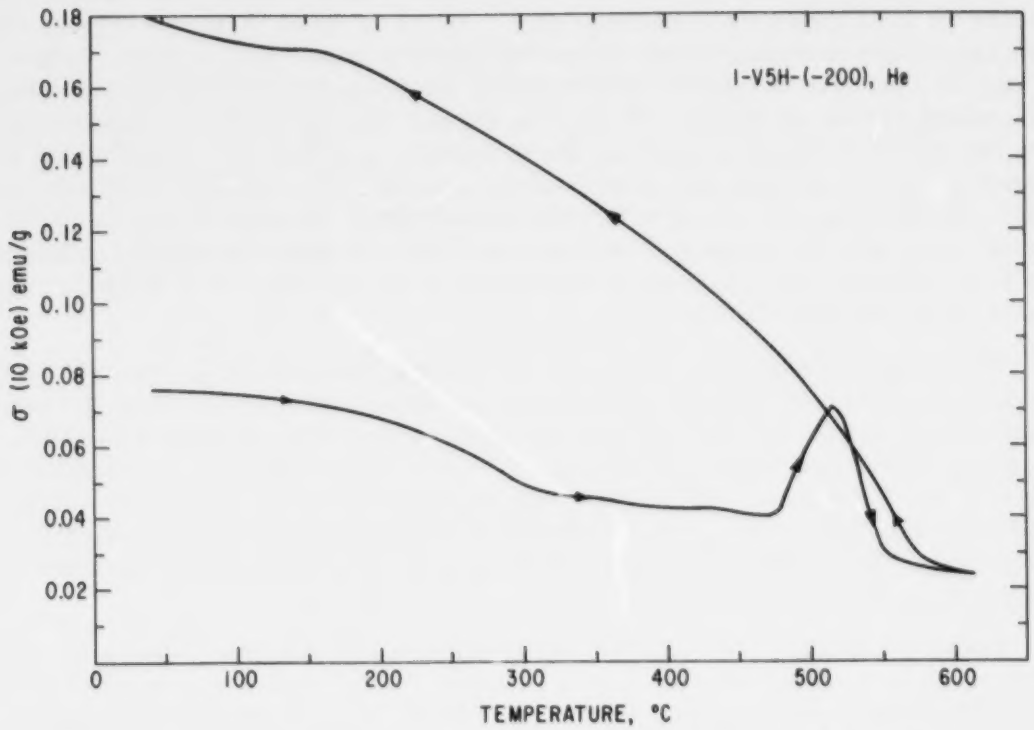

Figure 3. Thermomagnetic Behavior, σ vs. T, at 10 kOe in He Atmosphere of a Heavy Fraction from -200 Mesh Sample of Delmont Coal Piece. Average heating rate, 5°C/min.

It is tempting to speculate from this evidence that the pyrrhotite occurs with the pyrite (surface coating?) and facilitates the magnetic desulfurization.

The peak at 500°C is probably associated with a conversion to Fe_3O_4 from FeS_2 and perhaps from other iron-bearing minerals. The apparent Curie temperatures of 550° to 580° C are appropriate for high-iron spinels. The high value of σ obtained on cooling is typical for such a conversion.

In order to obtain a larger magnetization signal, low-temperature ashing (LTA) was used on some selected samples. The low-temperature ashing was carried out in an oxygen plasma at 145°C at the ERDA Morgantown Energy Research Center through the kind cooperation of W. F. Lawson, Jr., and J. J. Kovach. Samples of sieved coal, heavy fraction, and light fraction were tested by Mössbauer spectrometry and magnetization before shipping out for LTA. They were then reexamined on return.

There were three samples: whole coal, light fraction, and heavy fraction, all originally from a particular chunk (No. 2) ground to 100 x 200 mesh. Magnetization of the heavy fraction, No. 2-V2H, is reported in Table IX. Mössbauer spectra for all three samples are described later. The ash amounts after LTA are shown in Table X. These values are lower than expected,

Table X

ASH CONTENT AFTER LTA FROM 100 x 200 MESH SAMPLE OF CHUNK NO. 2 OF DELMONT COAL

Sample Fraction	Weight (% ash)
Whole	7.53
Heavy	75.80
Light	3.68

based on our previous chemical analyses of the homogenized Delmont coal. The magnetization data after LTA are also reported in Table IX in terms of grams of LTA ash and as calculated per gram of material before LTA.

The appearance of a significant σ_0 in the light-fraction post-LTA samples is a surprise: either it was present in the whole coal before LTA but escaped detection, or it represents a change produced by handling or by the LTA process. It is not a major component (cf. Mössbauer). It is amusing (coincidental?) to note that the post-LTA values on light and whole samples are similar in magnitude to those reported by Trindade (Thesis, MIT) on feed coal measured after LTA. Such data figured in his magnetic evidences for desulfurization, but the present results are anticorrelated with pyrites (expected to be more in heavy fraction). They do signify that a "paramagnetic" ash is concentrated by HGMS.

Thermomagnetic analysis of the light-fraction post-LTA material in helium (as for pre-LTA heavy fraction shown in Figure 3) displays a hint of a pyrrhotite Curie point near 300°C plus a larger fraction T_C near 490°C. The cooling data show a conversion to a high T_C (585°C) material, probably Fe_3O_4, and another lower T_C component (250° - 275 °C) suggestive of the cooling behavior of pyrrhotite.

STRUCTURAL AND CHEMICAL CHARACTERIZATION

The results of SEM and the associated energy dispersive analysis for representative heavy fraction particles and for an overview thereof appear as typical photographs and CRT traces in Figures 4 and 5, as well as in a more complete report in Table XI. Results from X-ray diffraction are also presented in the same table. The major work was on heavy fraction (100 x 200) material from coal chunk #1, divided up by passage through the Frantz Isodynamic (laboratory) Separator into Strongly Magnetic (I_H = 0.5 A), Moderately Magnetic (I_H = 1.0, 1.5 A), and Nonmagnetic. Some microprobe work on a light fraction from chunk #2 and on a polished chunk has also been done.

In the photographs there is an overview of the strongly magnetic fraction at 100X and of three individual particles at 500X that typify the major minerals

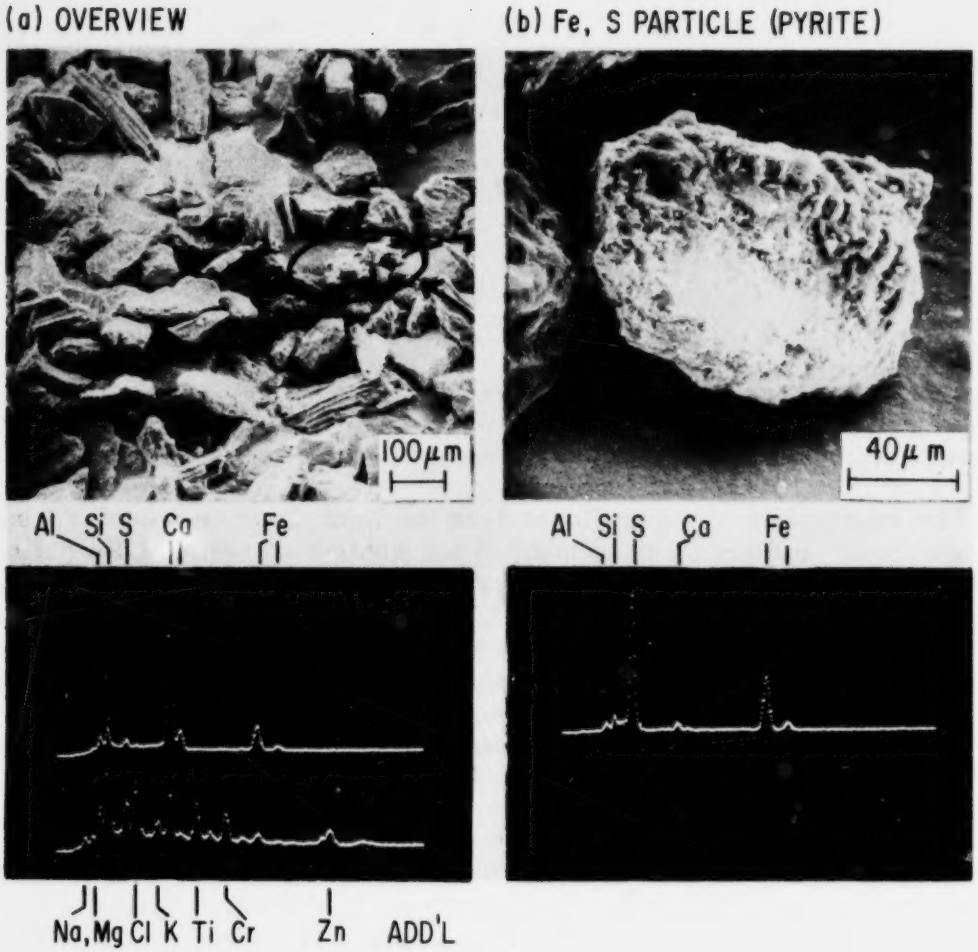

Figure 4. Scanning Electron Micrographs and Energy Dispersive Analyses of (a) Overview of Strongly Magnetic Particles and (b) Pyrite Particle from Powdered Delmont Coal. The lower analysis curve is for the circled cluster of particles with only the additional elements identified.

present (identified by their energy dispersive analysis traces and corroborated by overall X-ray results). These are as follows:

1. Fe, S particle; pyrite, FeS_2
2. Al, Si particle; kaolinite, $[(OH)_8Si_4Al_4O_{10}]$
3. Ca particle; calcite, $CaCO_3$.

In the table we report peak height intensity (arbitrary units) from the energy dispersive analysis for several individual pyrite particles, their ratio with respect to iron, and similar data for the three overviews taken with

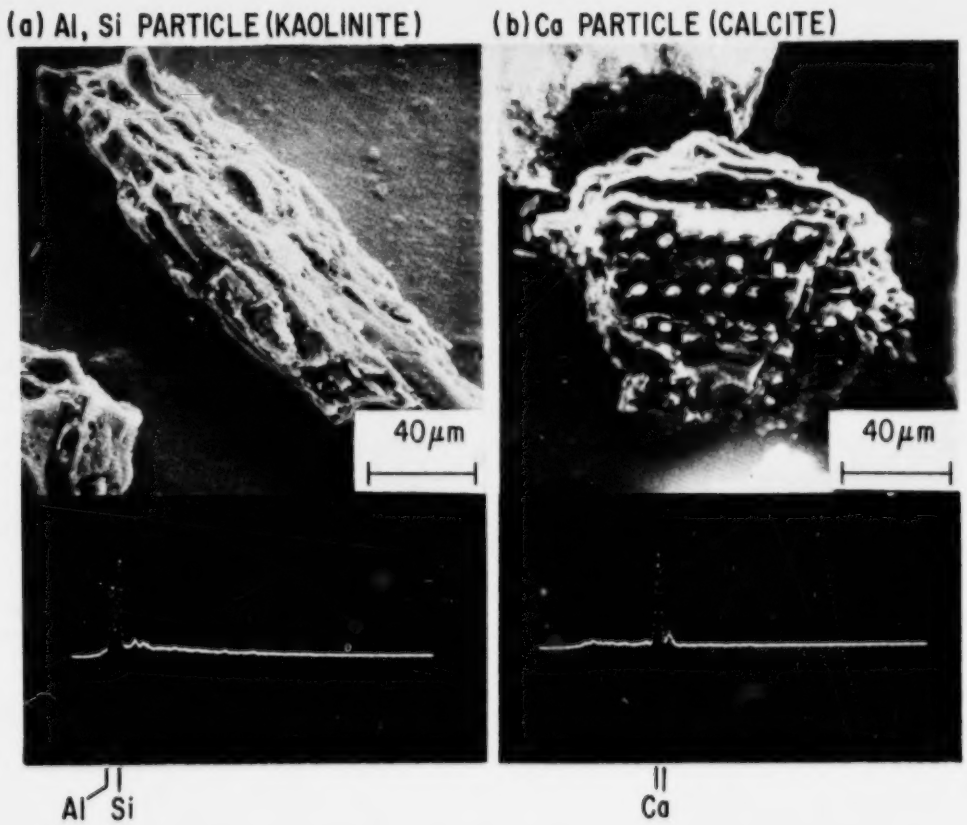

Figure 5. Scanning Electron Micrographs and Energy Dispersive X-Ray Analysis of (a) Kaolinite Particle and (b) Calcite Particle from Powdered Delmont Coal

equivalent conditions, so that comparisons among these latter are permitted. We note that, within a factor of about two, the peak height intensity roughly represents concentration. A number of comments may be made on these results:

1. The S/Fe ratio on the individual (presumably) FeS_2 particles sets a chemical scale. The ratio agrees to within 10% to 20% of a crude calculation of the intensity ratio for FeS_2.
2. The S/Fe ratio in the non-mag and mod. mag overview samples approximates that for FeS_2. For the strong mag overview sample the iron must be elsewhere (e. g., in the calcite-siderite phase).
3. Calcite-like minerals increase in importance as we go from non-mag to strong mag.
4. Clay minerals (Si, Al, K) have the inverse behavior to calcite-like minerals, but there seems to be a nontrivial clay carryover in the strongly magnetic portion.
5. For the cluster particle the high S/Fe is interesting but not understood.

Table XI

ENERGY DISPERSIVE ANALYSIS AND X-RAY DIFFRACTION RESULTS ON SELECTED SAMPLES OF DELMONT (UPPER FREEPORT) COAL[a]

	Peak Height Intensity (Arbitrary Units) and Ratio to Fe						
Sample	Fe	Ca	K	S	Si	Al	X-Ray Diffraction
FeS_2 particle in non-mag 1-H	11 (1)	--	--	31 (2.8)			NA
FeS_2 particle in mod. mag. 1-H	10.5 (1)	1.5	--	25.5 (2.4)			NA
Cluster particle in strong mag 1-H	1.8 (1)	8 (4.4)		7 (3.9)			EDA Also shows Na, Mg, K, Ti, Cr, Zn
Overview strong mag 1-H	5 (1)	27 (5.4)	--	2.3 (0.5)	4.5 (0.9)	3.5 (0.7)	$CaCO_3$, $(Me)CO_3$[b], $FeCO_3$
Overview mod. mag. 1-H	2 (1)	18 (9)	1.5 (0.8)	5 (2.5)	10 (5)	~7 (3.5)	35-40 vol% $CaCO_3$/$FeCO_3$ 25 vol% FeS_2 25 vol% Kaolinite; 10-15 vol% α-SiO_2
Overview non-mag 1-H	3.3 (1)	9 (2.8)	2 (0.6)	8 (2.5)	20 (6.2)	16 (4.9)	Kaolinite, $CaCO_3$, FeS_2
Light fraction 2-L				(see text)			Amorphous Carbon, Kaolinite (Weak), Some FeS_2
Light fraction 2-L; Post LTA							Kaolinite, $CaCO_3$, FeS_2 (pyr.), SiO_2, $CaSO_4 \cdot 1/2\,H_2O$, $FeCO_3$, FeS_2 (marcasite)

a) All samples from (100 x 200) size fraction.
b) $MeCO_3$, a (mixed ?) metal carbonate of intermediate lattice parameter between $CaCO_3$ and $FeCO_3$.

Additional materials characterization work on Delmont coal has the following results:

1. On a polished chunk of Delmont coal, SEM and X-ray maps of elements in Figure 6 show that pyrite particles are rather large (75 microns to ~300 microns). Small particles were not seen. This information is relevant to the liberation aspect of magnetic separation.

2. Some banding suggestive of clay minerals was also seen in Figure 6. Energy dispersive analysis of the banded regions confirms the presence of clay-mineral elements Al, Si, K, and some Fe. We are searching for coexistence of Fe with the clay mineral elements for the purpose of making more precise our knowledge of the origin of the "B" lines in the Mössbauer spectrum discussed in the next section. Calcite/siderite particles were not discerned, despite our evidence (X-ray and visual, on heavy fraction of ground coal) of their presence.

3. SEM and energy dispersive analysis on the light fraction (floats in CCl_4) of 100x200 mesh, ground Delmont coal reveals that each particle, more or less, shows some mineral content -- mostly clay and

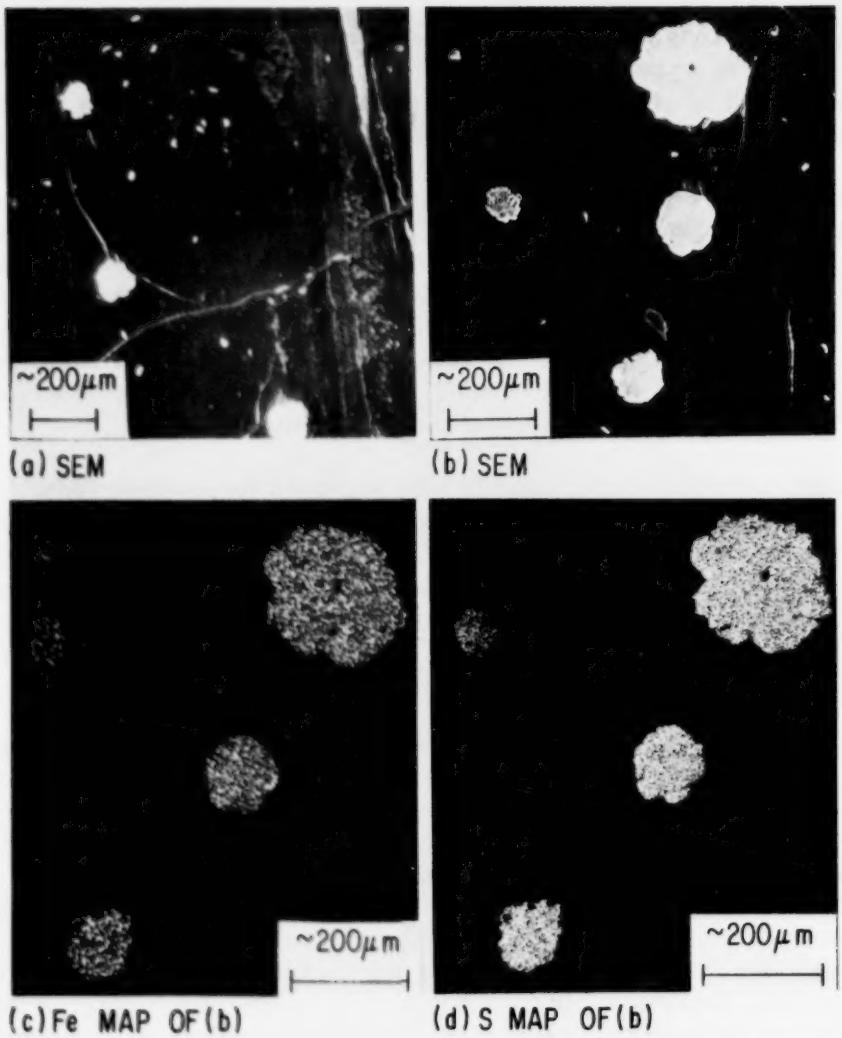

Figure 6. Scanning Electron Micrographs in (a) and (b) and X-Ray Maps in (c) and (d) of (b) for Fe and S, Respectively, on a Polished Surface of a Piece of Delmont Coal. The smallest specks are extraneous dust particles. The pyrite particles are ~100 μm up to ~300 μm in (b).

some pyrite elements. This agrees with X-ray data but tells us about the nature of the distribution. Typical element groups appearing are Al, Si, K, Ca, Fe and Al, Si, S, Ca, Fe, Cu.

4. X-ray analysis of the light fraction after LTA shows the minerals listed in Table XI in order of decreasing abundance.

MÖSSBAUER ANALYSIS

Mössbauer spectroscopy has been used under this contract because of its unique capabilities in characterizing the structural phases associated with iron. Consequently, it is also used here to analyze quantitatively for FeS_2. The Mössbauer spectrum (room temperature) of the Delmont coal shows two phases (see Figure 7). Phase A is conclusively identified as FeS_2. The absorption spectrum is a quadrupole-split doublet (lines A1, A2) corresponding to this weakly paramagnetic material. A second minor phase is identifiable. Line B2 presumably corresponds to the right-most pair of a quadrupole-split doublet. From the spectrum we know that the phase corresponding to lines B1, B2 is characteristic of a paramagnetic, strongly ionic, ferrous (Fe^{2+}) compound. Computer analysis of the spectrum would aid in the identification of the B compound, and we would be able to extract the relative fraction of the A and B phases (roughly proportional to line intensity).

A Fernglen anthracite coal sample was obtained for comparison. The spectrum of this anthracite shows a third phase (C1, C2) in addition to the FeS_2 and B phases evident in the Delmont coal (see Figure 8). Inasmuch as the pyrite content of anthracite coals is much less than in bituminous coals, the B and C phases appear to be present in larger relative quantity than the B phase in the previous sample. Lines C1, C2 correspond to another ferrous (Fe^{2+}) ionic, paramagnetic phase, more clearly identified below.

Three samples of (100 × 200) material were prepared from Delmont coal chunk #2: i.e., whole (sieved) coal, and the heavy and light fractions (sink-float in CCl_4). These same samples were sent for LTA at Morgantown. Their Mössbauer spectra at room temperature appear in Figure 9, normalized for equivalent pyrite absorption. The spectrum for whole coal closely resembles that shown in Figure 7. It shows clearly the quadrupole-split doublet A_1-A_2 characteristic of FeS_2 and the secondary line B_2 belonging to the as-yet-unidentified doublet. To our surprise the B_2 line almost disappeared in the heavy fraction, leaving a very weak line, C_2, whose existence on the shoulder of B_2 was suspected in some of our previous spectra. In complementary fashion, B_2 was considerably enhanced in the light fraction. In later work, carried out for quantitative evaluation, we observed a ten-fold increase of pyrites in the heavy fraction and a ten-fold decrease of pyrites in the light fraction, both with respect to the whole coal. Therefore, the enhancement (depression) of B_2 is largely apparent. In the light fraction B_2 is less than in the whole coal (about 1/4).

We are aware that the B_2 line has been studied in some depth in the only previously published Mössbauer investigation of coal we have been able to find.[36] From those results, we have indicated the position of its mate, B_1, which occurs very close to A_1 and consequently affects the "apparent" intensity ratio of "A_1": A_2. Lefelhocz et al.[36] made a very careful attempt to identify the B_1-B_2 doublet. It appears to be high-spin Fe^{2+} ion octahedral coordination. They leaned toward attributing its presence as "organic" iron

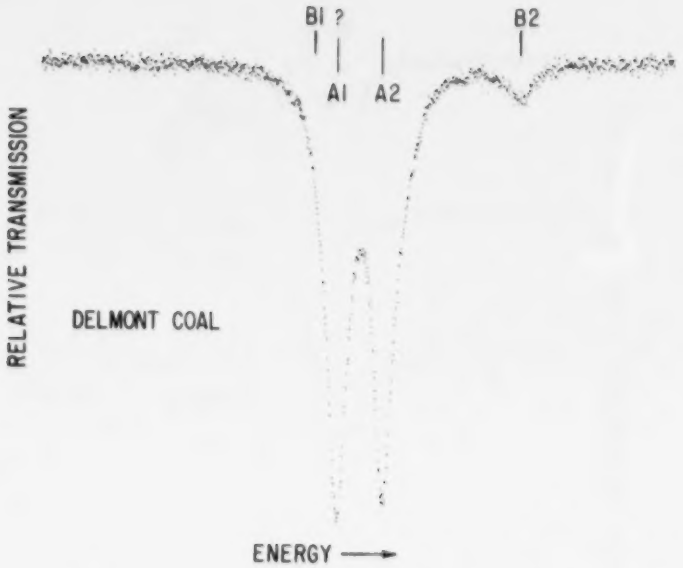

Figure 7. Mössbauer Spectrum from Delmont Coal at Room Temperature

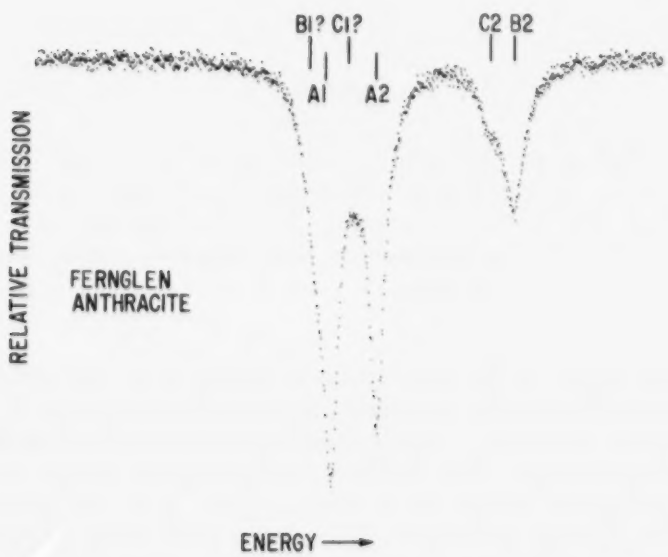

Figure 8. Mössbauer Spectrum from Fernglen Anthracite Coal at Room Temperature

in the coal macerals, but they could not completely exclude its association to a clay-like silicate mineral or gel. In our study we have tried to distinguish between these possibilities.

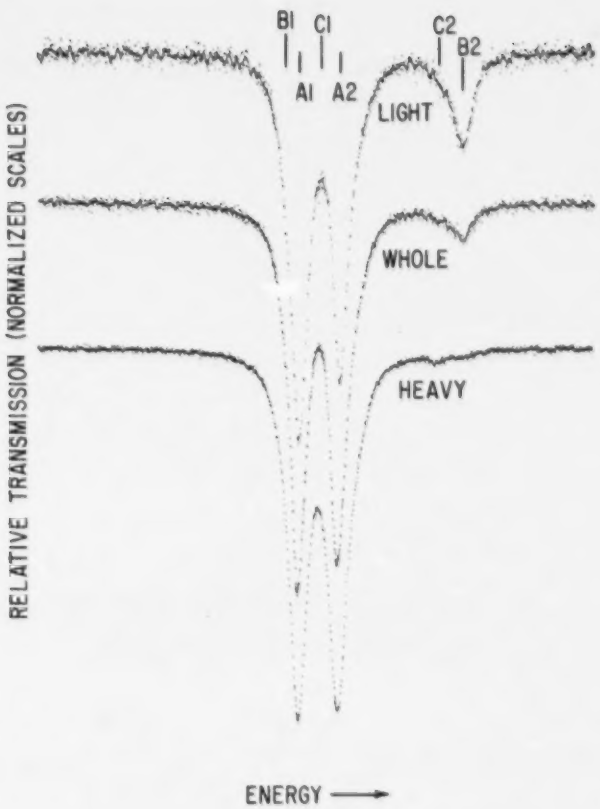

Figure 9. Mössbauer Spectra of a Sieved (100 x 200) Fraction of Delmont Coal Compared to Its Light and Heavy Components Separated by Sink-Float in CCl_4

In work outside this contract, we have found a strong enhancement of this B_1-B_2 line in a Pomeroy roof shale whose clay mineral content is higher than in usual coals. However, the crucial test should follow from the low-temperature ashing study. The Fe in a coal maceral would be profoundly affected by the oxidation of the coal, but the clay mineral should, in principle, remain unaffected by this process. Finally, if the Fe is organic and is oxidized by LTA, its new state could well affect the magnetization characterization of the coal fractions as well as their Mössbauer spectra. (As a high-spin Fe^{2+} ion, it contributes to the paramagnetic susceptibility.) We remark that the relative amount of Fe involved is not trivial (~10%) and that many previous magnetization studies of coal have been preceded by LTA.

The Mössbauer spectrum of each of the three samples after LTA is qualitatively similar to the pre-LTA results. (There are minor changes in

relative intensities of A_1-A_2, B_2-B_3, etc. spectra, but these may result from absorption effects.) From this measure it appears that there was no significant transformation of phases by the LTA process. This result is very important in the search for the origin of the B_1-B_2 doublet in the spectrum. It could not be organic Fe and remain unchanged. Hence, we lean more strongly to the suggestion that it is a finely divided or gel-like clay mineral containing Fe^{2+}

In Section IV, "Structural and Chemical Characterization," we noted several SEM observations on Delmont coal of the coexistence of Fe with elements normally belonging to clay minerals. These were in clay-like bands on a polished coal piece and on light-fraction particles (100 x 200). Thus, an identification of the B_1-B_2 doublet with a clay mineral containing Fe^{2+} is fully justified. Without going into detail on clay mineral compositions, our findings point strongly to the illite and chlorite groups of clay minerals.

At the later stages of this work, R. Hucko of the Bureau of Mines kindly helped us to locate references in contract reports and conference abstracts of some additional Mössbauer and SEM studies regarding iron-bearing clays in coal.[37, 38] These references were to work which followed that of Lefelhocz and others[36] in 1967 and which reached rather similar conclusions.

We also examined the three components of a preliminary HGMS water slurry run at MIT on Delmont Coal #7945, feed, mags, and tails; identified as run #4, 5-20, 64 kO_e. Their Mössbauer spectra are presented in Figure 10, normalized for equivalent pyrite absorption. Several results of interest are contained herein.

First, we note that the C_2 absorption line is present in the feed coal with intensity equal to B_2. In the mags, spectrum C_2 is enhanced and well defined, while it is suppressed in the tails, or product, spectrum. This absorption corresponds well to one of the doublet lines belonging to siderite ($FeCO_3$). Its mate, C_1, falls in the "valley" between A_1 and A_2, and can be inferred to be present by looking at peak-to-valley ratios. The association is reinforced by the SEM and X-ray evidence for the presence of calcite-siderite minerals in the Frantz Separator magnetic fractions (Table XI). Thus this paramagnetic component of the ash is also removed by magnetic separation. Finally, we have completed a justification for the attribution of the Curie-law behavior in the heavy-fraction magnetic susceptibility to a siderite-like mineral.

This series was also undertaken to attempt a semiquantitative analysis of the pyritic sulfur. By using equal amounts of sample in the same configuration, we hoped that absorption effects would be kept constant. As a rough approximation we used the peak height intensity (of A_2) as the measure, although the procedure is capable of refinement (area under line, etc.). The curves of Figure 10 have been normalized and are inapplicable in that form. From the direct data, we obtain the results shown in Table XII for the

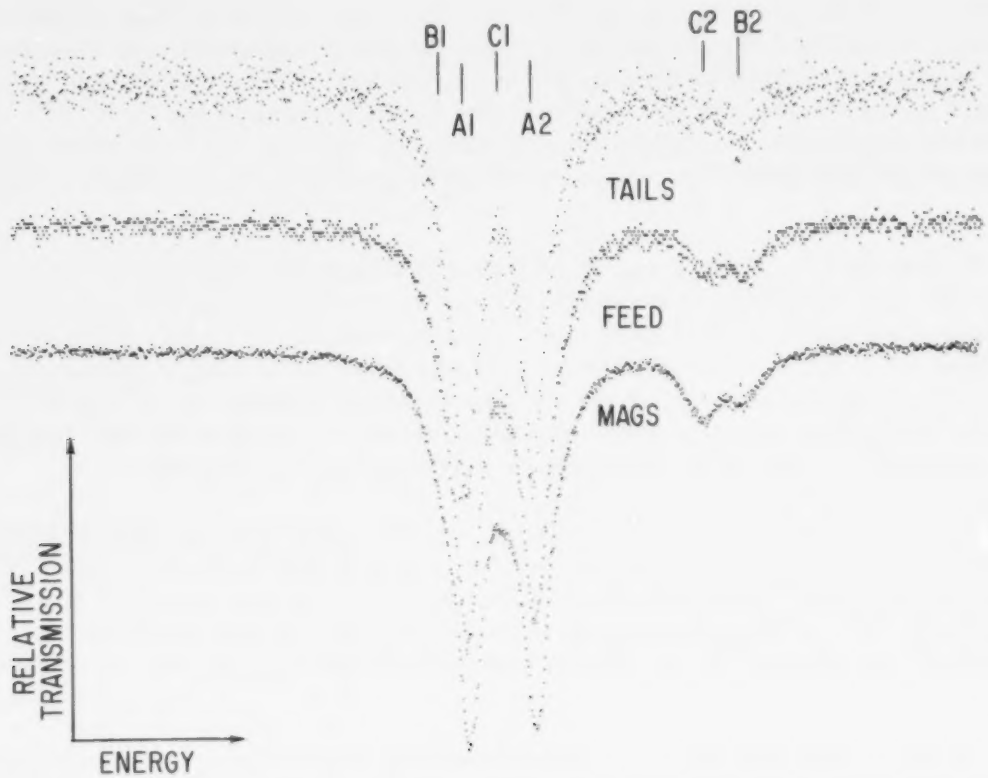

Figure 10. Mössbauer Spectra of the Feed, Mags, and Tails from the First Series of HGMS Runs: Sample #4

Table XII

MÖSSBAUER ANALYSIS FOR PYRITIC SULFUR IN FEED, MAGS, AND TAILS OF HGMS RUN #4 FROM FIRST SERIES OF TESTS, COMPARED TO CHEMICAL ANALYSIS

	Feed	Mags	Tails
Arbitrary units	0.034	0.059*	0.015
Normalized to feed analysis in wt. %	0.94	1.6	0.4
Chemical analysis in wt. %	0.94	1.41	0.26

*This value could be higher, owing to self-absorption effects at that level.

approximate relative concentrations of FeS_2 in the captured materials (mags) and in the product (tails). These are compared in the table to the direct chemical analysis.

The Mössbauer technique has also been tried in order to check on pyrite removal in the chemical analysis performed according to ASTM standards. Questions have been raised along this line by studies that show important concentrations of pyrite particles in the 1 to 10-micron-size range in certain coals. Our exposure to this question is from the work of Professor R. T. Greer of Iowa State University, who questions whether pyrite particles that are well encapsulated by coal can be leached by the dilute HNO_3 used for pyritic sulfur determination. Samples of the Delmont coal were obtained from EAC at various stages in their analysis for S, to see if the FeS_2 removal was as expected. Three samples were tested (1) untreated powder; (2) powder after HCl treatment, which should take out all of the Fe except that associated with FeS_2; and (3) powder after HNO_3 treatment, which takes out the FeS_2. Two samples of each were run. With the appropriate peak heights as an approximate measure of concentration, the results obtained are shown in Table XIII. It is clear that most of the nonpyritic iron is removed by the HCl treatment as expected (but not all), but more than 20% of the pyritic iron appears also to be removed! The HNO_3 treatment does remove essentially all of the remainder of the pyritic iron, as expected. We suggest that the Mössbauer technique could be used for quantitative analysis for pyrite in coal.

Table XIII

MÖSSBAUER ANALYSIS OF SAMPLES AT VARIOUS STAGES IN THEIR TREATMENT DURING SULFUR ANALYSIS

	Relative Heights of Peak			
	A2 for FeS_2		B2 for other Fe	
Sample	First Sample	New Sample	First Sample	New Sample
Untreated	4.2	4.5	0.8	0.9
After HCl	3.4	3.4	~0.2	~0.15
After HNO_3	~0.3	-	-	-

Section V

MAGNETIC SEPARATION OF COAL AS A WATER SLURRY

THE SEPARATOR SYSTEM AND EXPERIMENTAL METHODS

The 48 x 0 size fraction of the coal for the first series of experiments was slurried in water to a slurry density of approximately 10%. About 25 ppm of Alconox was used as a dispersant. Because the sample contained some rather large particles (~350μ), we used an expanded metal stainless steel matrix, rather than steel wool, to avoid possible clogging. A gravity feed system at constant head was used. In the first group of tests the nominal flow velocity was 1.5 cm/s and magnetic field strengths of 10, 20, 40, 60, and 80 kOe were used. In the second group of tests the field was held constant at 20 kOe and nominal flow velocities of 1.5, 3.4, 4.8, 5.6, and 11.6 cm/s were used. Two zero field runs were made at 3.4 cm/s. Both mags and tails were collected in each series of tests. The samples were filtered to separate out the solids. They were then dried and analyzed. A conventional canister and piping system with appropriate valving were used.

The tests were conducted by slurrying feed samples (150 to 200g) in a gallon of water. The slurry was continuously stirred just before use. The first five tests (samples 1 through 5) were run without a dispersant. The later tests were run with approximately 0.1g of Alconox added as the dispersant. The slurry was fed through the matrix by gravity; the flow was at constant head and was limited by an orifice in the exit tube. Because of the tendency of the slurry to settle out, water was added to the feed as the flow proceeded, so that the actual slurry volume passed through the matrix was usually 2 to 4 gallons. The net result is that, although the average superficial flow through the matrix was accurately determined, there were significant fluctuations in the slurry density during any single test. These were larger for the higher flow velocity measurements.

We also ran another set of tests on Delmont coal, tests similar in scope to the earlier set but with an improved technique to minimize materials losses in the system. (The general procedure is later illustrated in Figure 15.) The feed slurry was contained in a chamber directly over the matrix and was continually and vigorously stirred to promote sample uniformity. All of the feed sample was forced to enter the matrix. Flow rate was controlled by the size of the exit orifice and by maintaining constant head.

RESULTS AND ANALYSIS

In the first series of runs the material balance for both ash and sulfur was unsatisfactory. The difficulty was traced to material losses in the system. Two such losses could be accounted for in the following way: (1) small

fractions of the slurry feed that did not go through the separator and (2) a so-called "clean-out" fraction obtained by scouring the matrix after each magnetics product collection. Fortunately, these fractions had been saved. When they were analyzed separately for ash and total sulfur, rather high concentrations were found in the "slurry" fraction, evidently caused by gravity settling of the heavier particles. With these additional data, a better materials balance was obtained. Revised ash and sulfur concentrations for each feed sample can then be calculated by summing the ash and sulfur in all of the products, including the "slurry" and "clean-out" fractions. These calculated sulfur and ash concentrations are listed in Table XIV and are more realistic characterizations of the samples than those arrived at by summing the sulfur/ash in the mags and product fraction.

The following dilemma arises in interpreting the results of the first runs. If we calculate the sulfur/ash reduction using as the assumed feed composition, only that part of the sample which actually passed through the separator (i.e., excluding the slurry remnant) we are not fairly evaluating magnetic separation because the heavy slurry fraction, accidentally separated out, contains a significant amount of pyritic sulfur and ash. This result will yield an artificially low figure. An alternative calculation is to figure the reduction on the basis of the total sulfur/ash in the sample, including the slurry fraction in the feed. This is what would be obtained if all the sulfur/ash in the slurry remnant passed through the separator. The true value lies between these limits. In Table XIV we included the latter calculation.

To clean up the ambiguity arising from the presence of slurry remnants, we ran the second series of tests which avoided the problem by an improved technique of feeding the slurry. The results of these tests were in general agreement into the results of the first series of tests using the alternative method of calculation described above.

The numerical data of the analysis of ash and sulfur are shown in Table XIV and plotted in Figures 11 through 14 with the square symbols. The reduction in the pyritic sulfur is not plotted because of the uncertainties in the feed composition described above.

In all of the tests significant reductions were observed in the tails, i.e. the product, for both the pyritic sulfur and the ash. In most cases the total sulfur content could be reduced to below 1%. It is particularly noteworthy that the pyritic sulfur content of the tails goes down as the field is increased, the lowest being 0.22% at 85.5 kOe.

Three consecutive tails fractions were collected for sample 5, and these show the effect of loading. The first fraction has a pyritic sulfur content of 0.22%, the second 0.52%, and the third 1.16%. The ash content similarly increased from 5.0% to 6.3% to 8.6%.

Table XIV

DISTRIBUTION OF ASH AND SULFUR (FEED % CALCULATED) IN FIRST SERIES OF RUNS

RUN	H kOe	v cm/s	Feed wt. g.	Σ prod. wt. g.	% Ash in feed (calc)	% Ash in product	% Ash in mags	% Red. in Ash	% S_{TOT} in feed (calc)	% S_{TOT} in product	% S_{PYR} in product	% S_{ORG} in product	% S_{TOT} in mags	% S_{PYR} in mags	% S_{ORG} in mags	% Red. in S_{TOT}
1	10.69	2.80	158.0	156.5	9.7	6.5	21.4	33.0	1.07	0.96	0.50	0.46	1.80	1.56	0.24	10.3
2	21.38	2.80	178.0	173.2	10.9	6.2	23.0	43.1	1.57	0.92	0.46	0.46	1.91	1.54	0.37	41.4
3	42.75	2.80	161.8	160.4	11.2	5.6	22.4	50.0	1.59	0.78	0.33	0.45	1.70	1.41	0.29	50.9
4	64.13	2.80	137.5	135.1	9.6	4.3	20.8	55.2	1.57	0.70	0.26	0.44	1.87	1.41	0.46	55.4
5-1*	85.5	2.80	178.9	174.3	-	5.0	20.4	-	-	0.74	0.22	0.52	1.95	1.63	0.32	-
5-2	-	-	-	-	-	6.3	20.5	-	-	0.97	0.52	0.45	-	-	-	-
5-3	-	-	-	-	-	8.6	-	-	-	1.47	1.16	0.31	-	-	-	-
5†	-	-	-	-	10.7	5.57	20.5	47.9	1.51	.84	0.35	0.49	1.95	-	-	44.4
6	42.75	2.80	141.1	140.4	10.8	5.5	27.0	49.1	1.18	0.70	0.26	0.44	2.51	2.27	0.24	40.7
7	42.75	2.80	145.8	142.4	11.0	5.8	26.1	47.3	1.44	0.77	0.30	0.47	2.39	.96	1.43	46.5
8/9	21.38	1.51	213.0	204.0	10.3	5.7	19.9	44.7	1.58	0.77	0.36	0.41	1.80	1.41	0.39	51.3
10/12	21.38	3.26	203.6	197.6	11.1	5.7	35.4	48.6	1.59	0.81	0.38	0.43	3.54	2.97	0.57	49.1
11/13	21.38	4.55	216.9	215.9	10.8	9.0	38.1	16.7	1.33	1.08	0.71	0.37	2.41	2.29	0.12	18.8
14/15	21.38	5.86	199.3	195.0	11.1	9.9	32.7	10.8	1.45	1.14	0.84	0.30	2.32	1.47	0.85	21.4
16/17†	21.38	9.80	155.0	172.9	10.6	9.7	45.6	8.5	(1.28)	1.04	-	-	-	-	-	-
18/19	0	1.74	202.2	190.4	10.7	10.3	13.1	3.7	1.19	1.04	0.68	0.36	2.22	1.95	0.27	12.6
20/21	0	2.98	226.4	222.6	11.0	10.5	16.2	4.5	1.26	1.12	0.81	0.31	2.85	2.53	0.32	11.1

* 3 consecutive samples
† Weighted average of the three

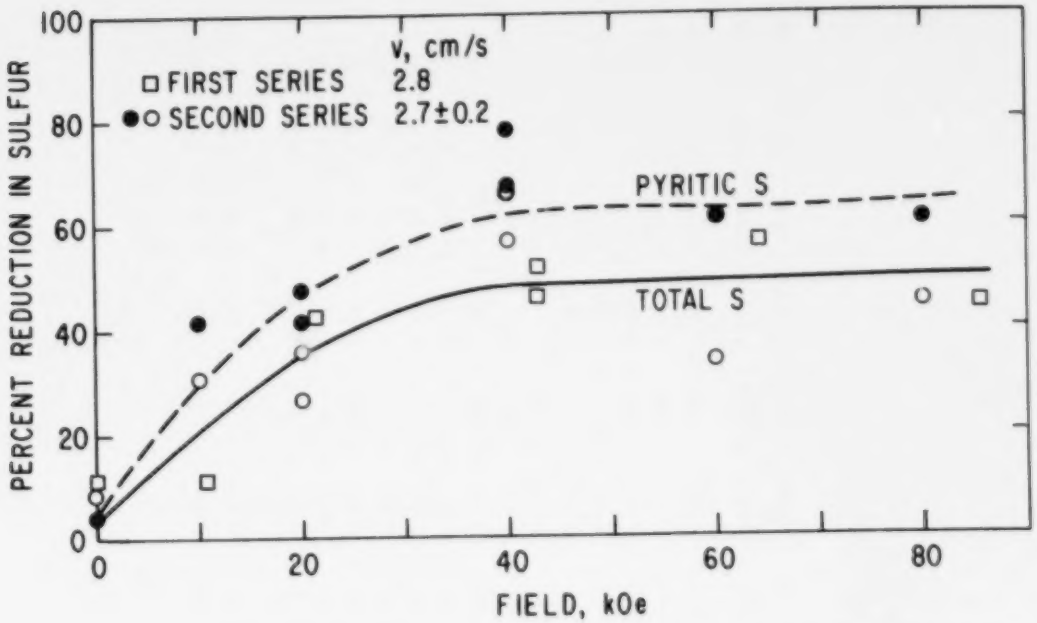

Figure 11. Sulfur Reduction as a Function of Field from Both Series of Runs in the HGMS Apparatus. Solid points are pyritic S data.

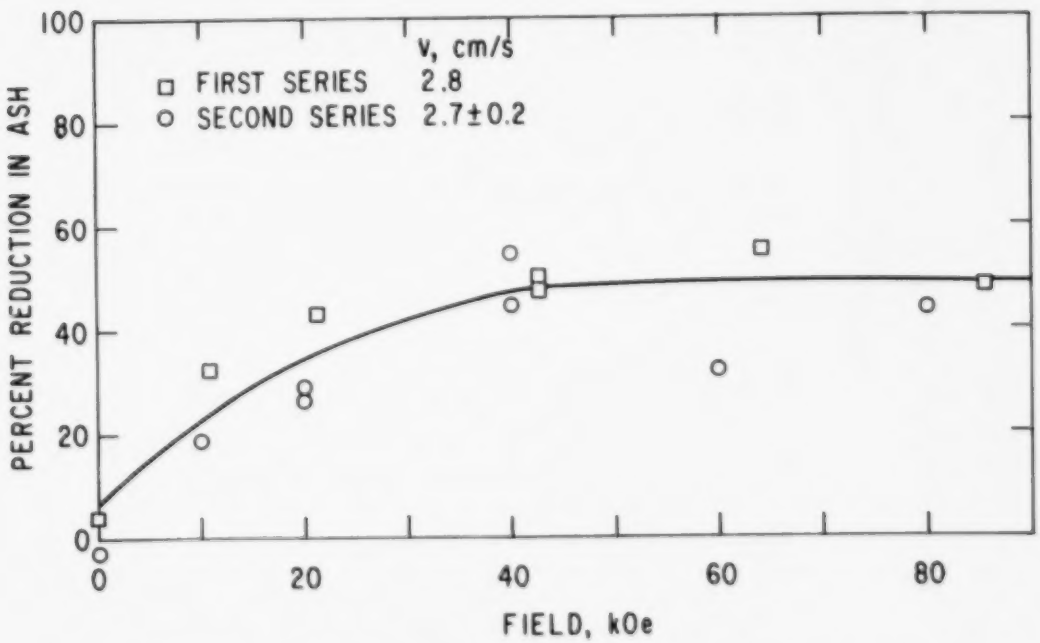

Figure 12. Ash Reduction as a Function of Field from Both Series of Runs in the HGMS Apparatus

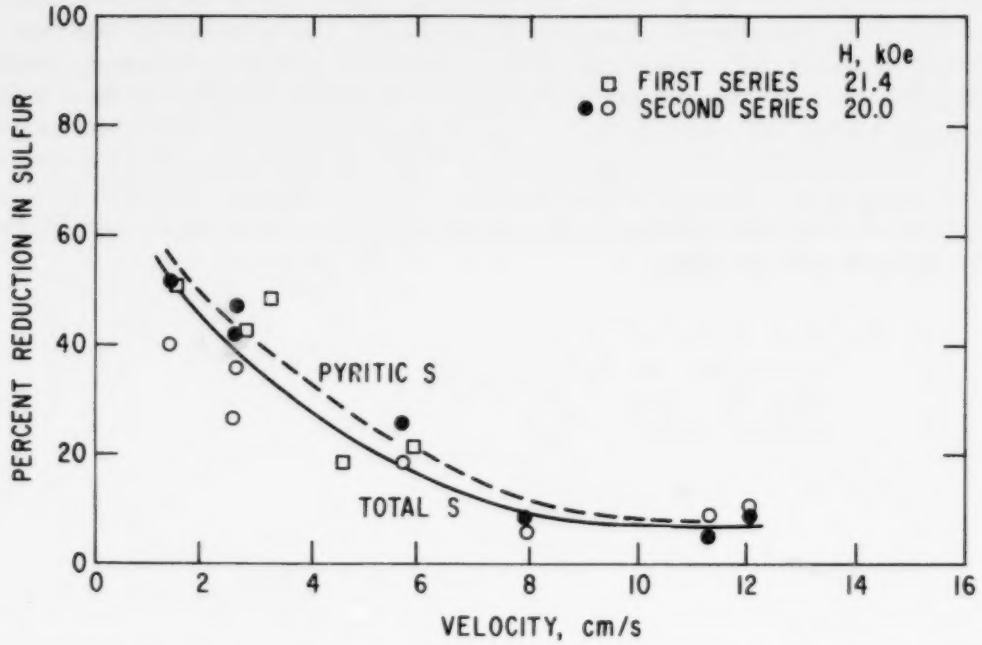

Figure 13. Sulfur Reductions as a Function of Velocity from Both Series of Runs in the HGMS Apparatus. Solid points are pyritic S data.

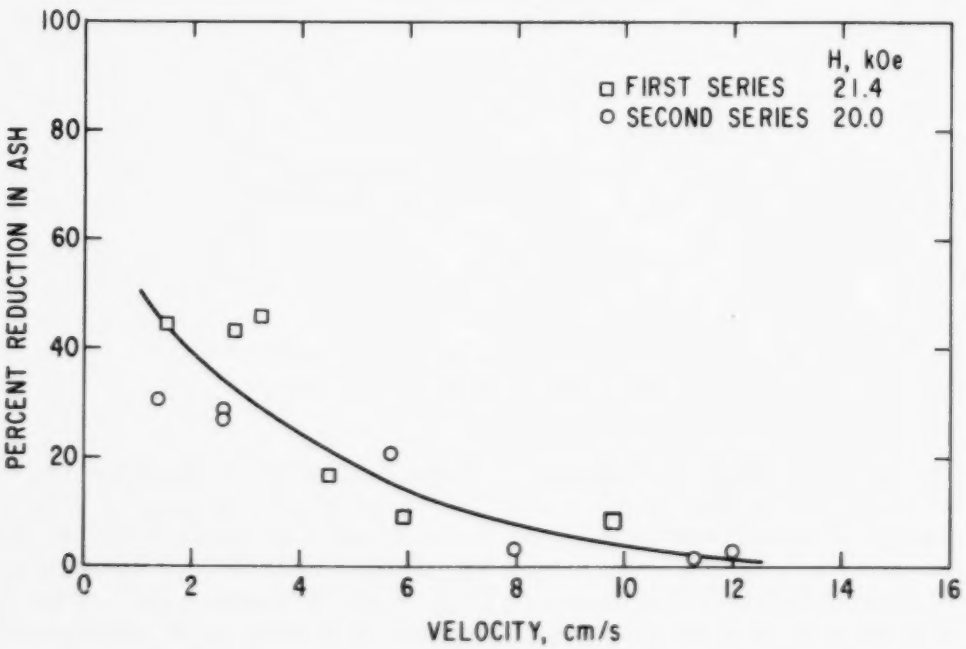

Figure 14. Ash Reduction as a Function of Velocity from Both Series of Runs in the HGMS Apparatus

In the second series of tests the material balances were greatly improved by using the system shown in Figure 15. The numerical results are presented in Table XV. Because of the improved material balance, these results show reasonable trends when plotted directly as total sulfur, pyritic sulfur, and ash in the product (i. e., tails) as a function of field and velocity. These results are shown in Figures 16 and 17. In addition, these results are plotted as the reduction in total sulfur, pyritic sulfur, and ash in Figures 11-14 as they are for the first series of tests. The agreement between the two sets of data is good.

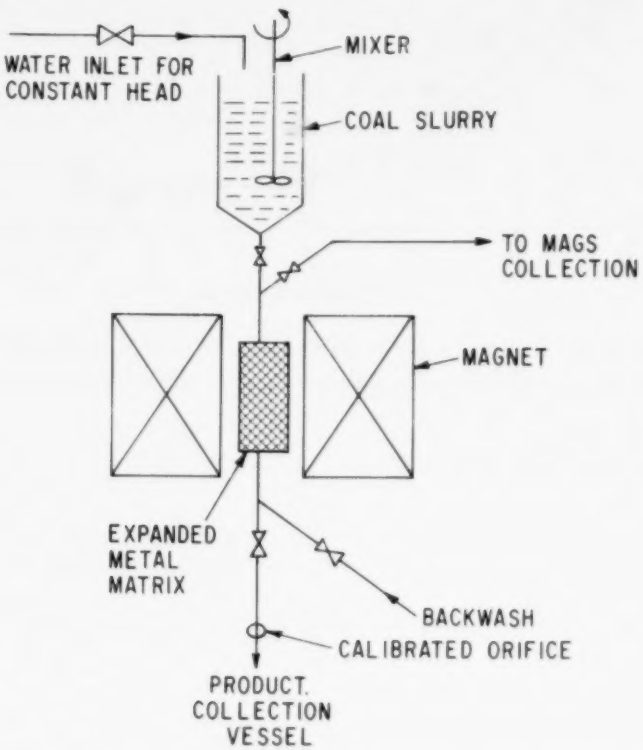

Figure 15. Magnetic Separation Apparatus for Second Series of Tests

Calculations by means of the physical model described in an earlier section were carried out. In order to apply this model to the case of coal separation, we have chosen the set of parameters listed in Table XVI. In addition, only collection on the front edge of the stainless steel fibers was considered because of recent direct observations, [28, 33] which showed that collection on the downstream side of the fibers was not significant. The dimensions and saturation magnetization of the expanded metal used in the HGMS collecting can were measured directly. The magnetic susceptibility of the coal phases are average values deduced from our measurements as summarized

Table XV

SECOND SERIES OF HGMS RESULTS ON WATER SLURRY

#	H kOe	v cm/s	PRODUCT % Ash	PRODUCT % S_{TOT}	PRODUCT % S_{PYR}	PRODUCT % S_{ORG}	MAGS % Ash	MAGS % S_{TOT}	MAGS % S_{PYR}	MAGS % S_{ORG}	% Red. Ash	% Red. S_{TOT}	% Red. S_{PYR}
1	20	2.60	12.1	1.02	0.69	0.33	41.3	3.73	2.55	0.88	28.4	35.4	46.9
2	40	2.44	7.7	0.68	0.29	0.39	43.9	3.36	3.21	0.15	54.4	57.0	77.7
3	40	2.93	9.4	0.52	0.42	0.40	44.0	3.92	3.62	0.30	44.4	67.1	67.7
4	10	2.74	13.7	1.10	0.76	0.34	37.0	3.68	3.29	0.39	18.9	30.4	41.5
5	60	2.53	11.5	1.05	0.50	0.25	36.6	3.18	2.56	0.62	32.0	33.5	61.5
6	80	2.93	9.5	0.88	0.51	0.37	40.8	3.40	2.87	0.53	43.8	44.3	60.8
7	0	2.62	17.5	1.44	1.24	0.20	27.6	4.70	4.39	0.31	-3.6	8.9	4.6
8	20	1.36	11.7	0.95	0.63	0.32	37.3	3.37	2.84	0.53	30.8	39.9	51.5
9	20	2.55	12.4	1.16	0.76	0.40	34.4	3.48	3.17	0.31	26.6	26.6	41.5
10	20	5.67	13.4	1.29	0.97	0.32	55.1	4.92	4.81	0.11	20.7	18.4	25.4
11	20	7.94	16.4	1.50	1.29	0.21	61.6	4.52	3.78	0.72	3.0	5.1	0.8
12	20	11.33	16.7	1.44	1.24	0.20	47.5	2.86	1.92	0.94	1.2	8.9	4.6
13	20	12.03	16.4	1.41	1.19	0.30	59.0	4.60	3.53	1.07	3.0	10.8	8.5
14	40	1.40	9.5	0.82	0.40	0.42	42.8	2.60	3.19	0.41	43.8	48.1	69.2
15	80	1.28	10.6	0.94	0.78	0.16	33.8	2.94	2.32	0.62	37.3	40.5	40.0
16	0	1.35	16.2	1.21	0.83	0.38	32.1	5.22	4.54	0.68	4.1	23.4	36.2

Feed Analysis

Ash	16.9%
Total S	1.58%
Pyr. S	1.30%
Org. S	0.28%

TABLE XV
SECOND SERIES OF HGMS RESULTS ON WATER SLURRY

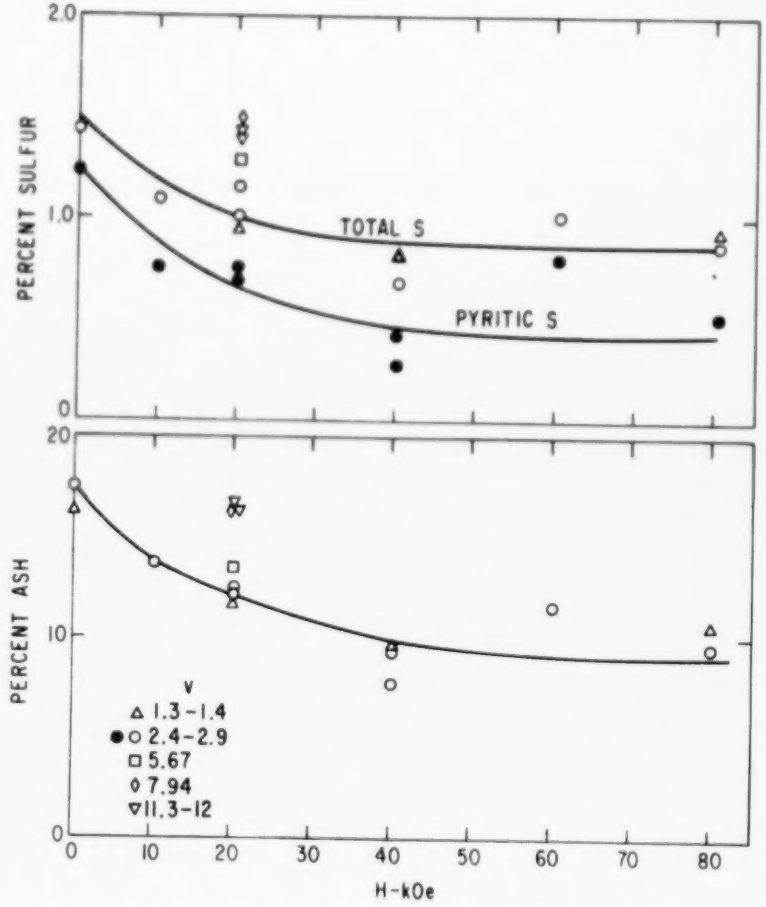

Figure 16. Sulfur and Ash in the Product as a Function of Fluid Velocity for a Variety of Applied Fields—Curves Drawn Through Data for 20 kOe; Second Series of Runs

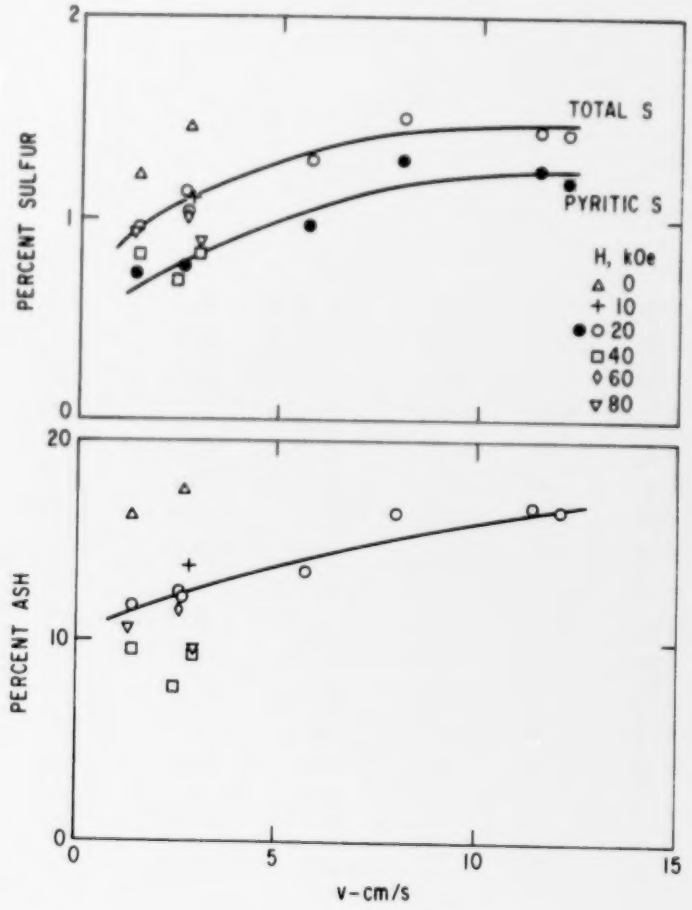

Figure 17. Sulfur and Ash in the Product as a Function of Applied Field for a Variety of Fluid Velocities—Curves Drawn Through Data for $v \approx 2.7$ cm/s; Second Series of Runs

Table XVI

INPUT PARAMETERS FOR CALCULATIONS

FEED

		COAL	SULFUR	ASH
w_d	Total wt., g	175		
	wt., %		1.4 (S)	10
w_p	wt., g		4.59 (FeS_2)	17.5
ρ_p	density, g/cm^3	1.3	5.0 (FeS_2)	2.1
χ_m	magn. susc., emu/cm^3	-0.6×10^{-6}	$[0.075/H] + 10^{-5}$	$[0.5/H] + 25 \times 10^{-6}$
P Size, μm				
	50%	220		
	25%	110		
	25%	20		

FILTER CAN

L	length, cm	11.9
	cross section, cm^2	15.6

FILTER FIBERS

W	total wt, g	150
	$4\pi M$, G	17,800
T	thickness, μm	580
S	width, μm	740
ρ_f	density, g/cm^3	7.86
a	active radius curv., μm	400

FLUID

η	viscosity, poise	10^{-2}
χ	magn. susc., emu/cm^3	-0.7×10^{-6}
ρ	density, g/cm^3	1.0

in Table IX. The particle size distribution shown is an approximation of the measured size distribution of the feed given in Table VIII. For simplicity and because of the large scatter in the data, we assumed that the mechanical capture was zero. We then calculated the filter efficiency normalizing factor, f, to obtain a fit to the experimental results for both S and ash at v = 2.8 cm/s and H = 21.4 kOe, assuming complete liberation of the magnetic phases from the diamagnetic coal and assuming a single particle size of 220 μm. The calculated curves as a function of v and H were then obtained and are shown by the solid curves in Figures 18 to 21. Note that the values of f for both sulfur and ash are close to each other but more than a factor of 10 smaller than deduced from the CuO/Al_2O_3 results. (29, 31)

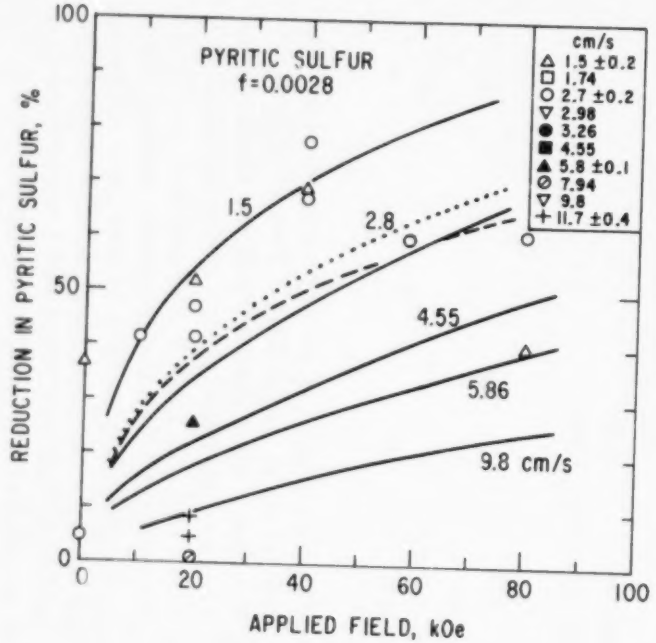

Figure 18. Calculated Curves and Experimental Data for Pyritic Sulfur Reduction as a Function of Field. Solid curves calculated for particle size of 220 μm using the parameters shown in Table XVI - dotted curve calculated for an assumed distribution of liberated particles, 50% fully liberated and 50% half-liberated; dashed curve calculated assuming particle size distribution given in the table.

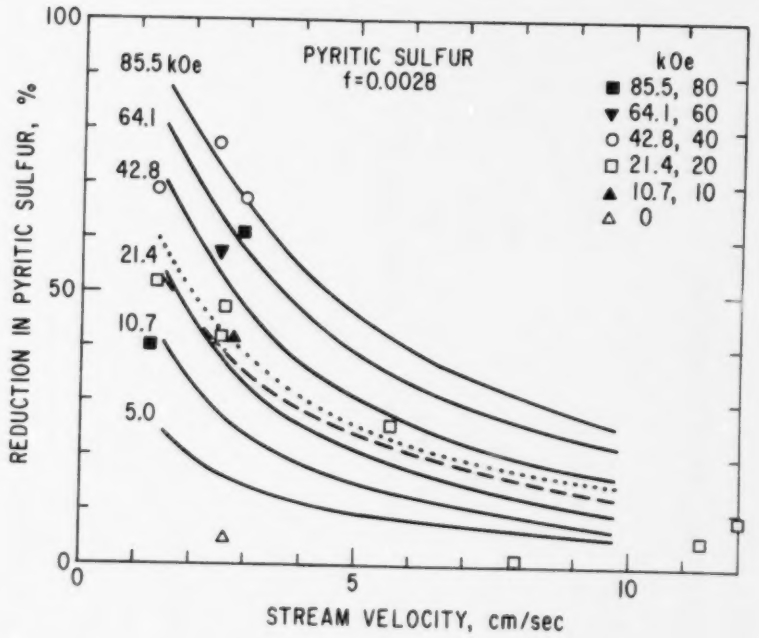

Figure 19. Calculated Curves and Experimental Data for Pyritic Sulfur Reduction as a Function of Velocity, as Described in Figure 18 Caption

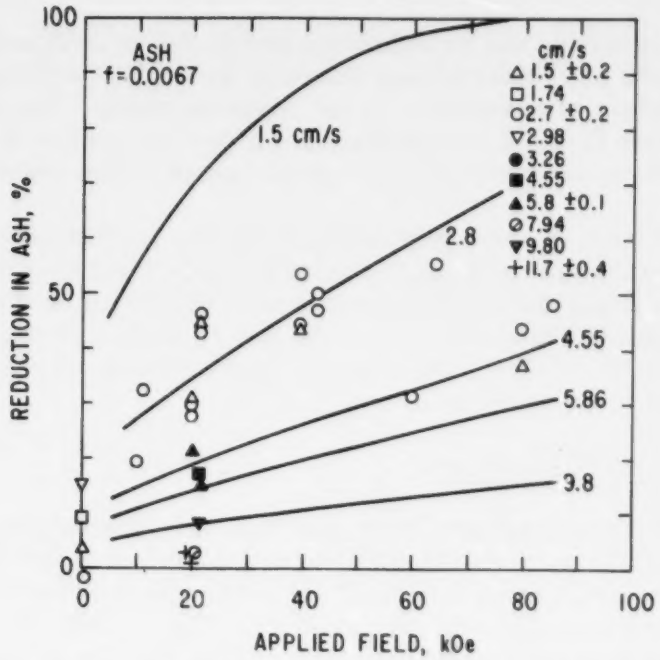

Figure 20. Calculated Curves and Experimental Data for Ash Reduction as a Function of Field

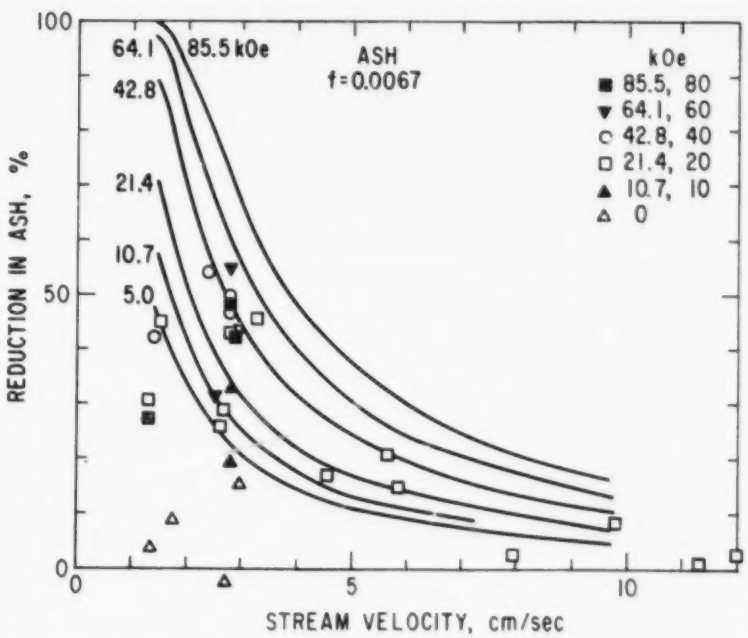

Figure 21. Calculated Curves and Experimental Data for Ash Reduction as a Function of Velocity

To see how sensitive the calculations are to the size distribution, we included the simple size distribution listed in Table XVI without changing f or the active radius of curvature, a (or anything else). The results calculated for only one H and v are shown by the dashed curves in Figures 18 and 19. The difference is not very dramatic but is in the right direction.

We then assumed an arbitrary function for the liberation of the magnetic phases from the diamagnetic coal phase: 50% fully liberated and 50% half-liberated. Again using the single particle size of 220 μm and without any changes, we calculated the effect at one H and v, shown by the dotted curves in Figures 18 and 19. Except for a small displacement, the functional dependence appears to be unchanged.

DISCUSSION AND CONCLUSIONS

It is clear that the magnetic field and flow are affecting the removal of pyritic sulfur and ash minerals in approximately the manner expected. Increasing field and decreasing flow both increase the recovery of the magnetic phase leading to a cleaner coal product. The model calculations can be made to fit the data only approximately. This may be in part a result of the large scatter in the results, especially for the pyritic sulfur. The effect of the size distribution and degree of liberation assumed in the calculation appeared to be minor.

In the case of the recovery of the ash, there appears to be a much smaller observed field and flow dependence than calculated. This may be accounted for by assuming that a large fraction of the ash minerals are non-magnetic: approximately 30%.

The experimental scatter seen here is certainly very much larger than observed in the CuO/Al_2O_3 model system[22, 23] and may be attributable to the variability in the coal from sample to sample.

Section VI

MAGNETIC SEPARATION OF COAL AS A DRY POWDER

SEPARATOR SYSTEM AND EXPERIMENTAL METHODS

The air system for the magnetic separation of coal is shown schematically in Figure 22. Our first attempts to use a screw feeder for the coal were successful with a distribution containing relatively coarse particles, but they were unsuccessful on the 60 x 0 fraction, which contained many fines. The fine coal had a tendency to pack, making the screw feeder inoperative. We therefore devised a simple vibratory shaker type of feeder, which circumvented this difficulty. Although the feed rate is not as uniform as it would be with an operative screw feeder, this does not seem to be a problem. On the other hand, because it is a simple batch device, we can determine the mass of the feed sample very accurately and have been able to achieve an overall mass material balance of the order of 1% or better. The first tests were made with a canister 1 inch in diameter and 6 inches long.

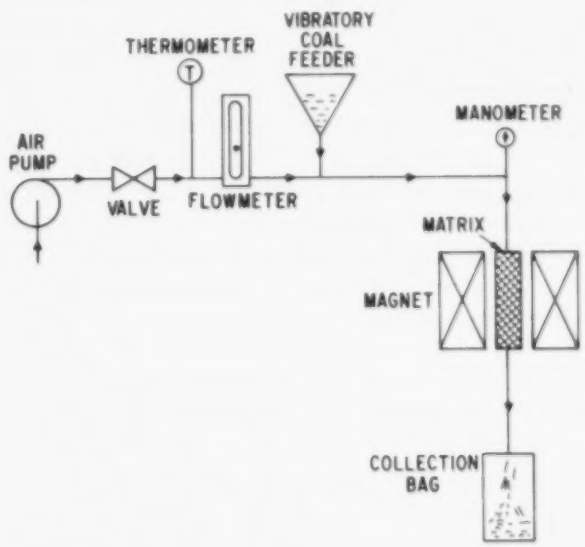

Figure 22. Air System for Magnetic Separation of Dry Coal

In the preliminary tests it was shown that very good material balances were achieved. However, the preliminary tests did not demonstrate any significant reduction in the sulfur and ash content of the products. There is definite evidence of magnetic differentiation between the mags and the product, but it is overshadowed by another effect, which we at first believed to be electrostatic charging of the particles and subsequent agglomeration. Tests were made both in a field and in zero field. Although there is an increase in the ratio

in the presence of a field, the effect is small. Also the separation efficiency does not improve with increase in H/v. However, there are sufficient data points above the range of zero field separation to give us confidence that sulfur and ash are being separated magnetically in spite of the fact that some other phenomenon is interfering. These tests were made mostly with an expanded metal matrix in the canister; a few were run with stainless steel wool.

RESULTS OF HGMS ON DRY COAL POWDERS

In contrast to the successful magnetic separations performed on water slurries of coal, the dry separations were disappointing. Although some degree of magnetic selectivity was observed, we were not successful in this limited test program in achieving separations at all comparable to those obtained with the water slurries. Several hypotheses for this have been advanced, but in the limited time remaining for this work we could not test them adequately. Following is a description of the tests, the results, and the tentative conclusions we have drawn.

The first series of tests was run with a canister one inch in diameter and 6 inches long with an expanded metal matrix similar to that used in the water tests. The feed material was Delmont 60 x 0 reconstituted from separate 2 x 1/4, 1/4 x 48, 48 x 0 fractions in the proportions that these fractions had been derived from the original coal. Fifteen runs were executed with fields which varied from 0 to 80 kOe and superficial air velocities of 32 to 915 cm/s. The reduction in the sulfur content of the product over that of the feed was small and irregular, rarely more than 10 percent and sometimes imperceptible. A more positive indication that some magnetic separation was taking place was that the sulfur (and ash) content of the mags was always definitely larger than that of the product. (These data will be presented graphically later in this discussion.)

In the next series of 24 tests we substituted coarse steel wool for the expanded metal in the matrix canister. Magnetic fields up to 50 kOe and air velocities of 59 to 1,018 cm/s were used. In several of these tests the products were passed through the matrix anywhere from 2 to 4 times. No substantial improvement in the sulfur or ash reduction was noted in these tests either. We suspected that electrostatic charging effects were occurring and grounded the matrix but with no improvement. In these tests, however, as in the preceding series, we again noted an enhancement in the sulfur and ash content of the mags as compared to the product.

To further explore the possibility that electrostatic effects might be present, we performed a simple experiment to see if the agitation of the coal in the glass feed flask put a charge on the coal. After shaking in the flask we placed a few grams of the coal on the electrode of an electroscope. A clearly detectable charging effect was observed although the experiment was only qualitative.

We then replaced the glass flask by a metal flask and made sure that all parts of the system were at the same potential by interconnecting and grounding. Seven more runs were performed with this arrangement, again with no significant change in the results. We concluded that the major problem was not electrostatic charging.

A batch of 60 x 0 Delmont coal was next washed in methanol, filtered, and dried. The assumption behind this was that the coal particles might be coated with some foreign organic material causing them to agglomerate and the methanol could possibly remove this coating. Again no substantial improvement was observed.

In the next series of tests we tested a batch of 60 x 100 Delmont coal which had been produced by splitting off the -100 fraction. We also split off a 60 x 400 fraction. Again the product was not significantly improved, but the enhancement of sulfur and ash in the mags was somewhat greater than in preceding runs.

We then ran a test using the mags that had been collected in some of our earlier water slurry tests as a feed material. These were, of course, dry. The purpose of this test was to test the idea that some alteration of the pyrite takes place in the water slurry enhancing the magnetic properties of the pyrite. Because we had relatively little material to work with, we could not do extensive testing. In these runs we found that in a field of 20 kOe and a velocity of 59 cm/s, 74 percent of the feed was trapped as mags. In zero field we observed trapping of 23% to 46%. This shows that the magnetic fraction we successfully captured in a water slurry could also be captured in an air stream, although not as completely. A sizable zero field capture also occurred. It should be noted that this high trapping percent occurred with previously beneficiated material, i.e., there were few coal particles to promote the undesirable agglomeration hindering magnetic separation.

To determine whether or not the water had converted the pyrite in the coal to a more magnetic form, we slurried some Delmont 60 x 400 coal in water and let it stand for 12 1/2 hours in one case and 84 hours in another. (This, of course, was a much longer period of time than the few minutes the coal had been immersed in the original water slurry tests.) The coal was then dried and injected into an air stream and fed into the magnetic separator at a field of 20 kOe and a velocity of 59 cm/s. The results were disappointing. No significant difference was observed between the mags and the product.

The result of all these tests is best summarized in the two accompanying plots, Figures 23 and 24. We have plotted the ratio of the percent sulfur (or ash) in the mags to the percent sulfur (or ash) in the product, for each test run, vs. the parameter H/v. This separation parameter was easier to use experimentally (in contrast to the product/feed ratio) because of the marginal beneficiation. There is no significant correlation with H/v; however, the plots are useful in setting off those data for which the ratio is noticeably

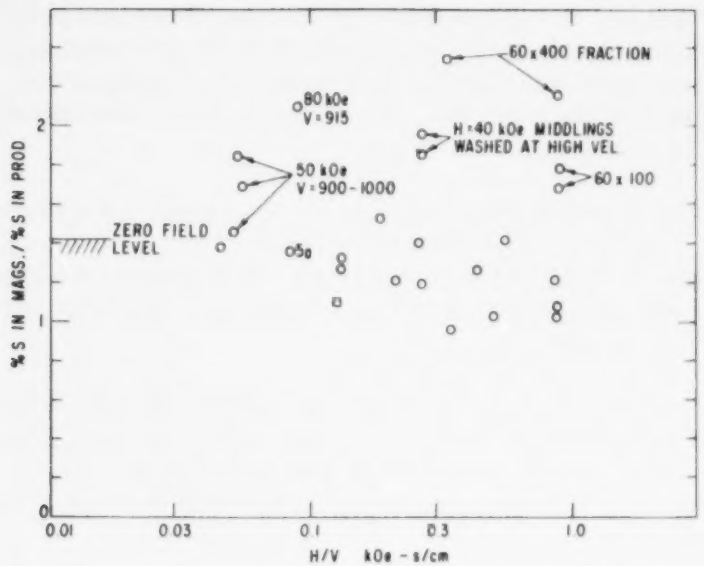

Figure 23. Ratio of Ash Collected in Mags to Ash in Product as a Function of (Field/Velocity) for Dry Powder Separation

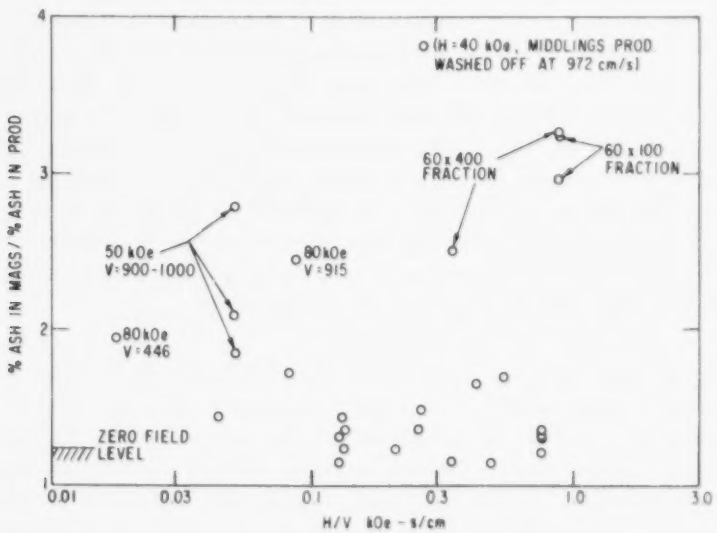

Figure 24. Ratio of Sulfur Collected in Mags to Sulfur in Product as a Function of (Field/Velocity) for Dry Powder Separation

larger than the zero field background. These are, first, the runs in which the fines were split off and a few others in which a high field in combination with a high flow velocity was used. Generally the fraction of mags collected ranged from 50% to 10%, decreasing with increasing velocity, but showing rather little field dependence as well as rather little correlation with sulfur (ash) content.

CONCLUSIONS AND DISCUSSIONS

Our conclusions at this stage are as follows:

(1) We have achieved only marginally observable desulfurization in air streams.

(2) The presence of fines -400 (or -100) impede magnetic separation, possibly because they act to promote agglomeration of coal and pyrite.

(3) Our admittedly limited test gave no indication that the magnetic properties of the pyrite were enhanced by water immersion, but these tests were not extensive enough to provide a final answer.

The question of why wet magnetic separation was successful and dry separation thus far unsuccessful has not been definitively answered. It may be that local turbulence of the air stream occurs in the vicinity of the individual matrix fibers and that the viscous forces for this reason are much greater in air than in water. We have also not definitively determined whether or not chemical alteration of pyrite occurs in water. To answer these questions some further testing is required.

To determine if there are inherent difficulties with dry separation because of exaggerated viscous forces arising from turbulence, we could look at a system like a mixture of Al_2O_3 and CuO which has been previously studied in water slurries and for which data is available. Performing a dry magnetic separation on this system, whose constituents have known magnetic properties, will provide us with data we can compare directly to the water slurry results.

These tests should be supplemented with more extensive tests on coal which has been treated in water of controlled pH. In addition, both magnetic susceptibility and Mössbauer measurements should be performed on coal so treated, to decide more definitively if the magnetic properties are altered by water treatment.

Section VII

RECOMMENDATIONS

1. Given the background information we have developed on the performance of water slurries of this coal, and the characterization of this coal, we have a unique opportunity to try to understand the reasons for the poor performance of this coal as a dry powder. We recommend further work to explore this problem.

2. We have demonstrated, on another coal in a water slurry, the ability of high gradient magnetic separation to remove most of the pyritic sulfur and a substantial fraction of the ash. We recommend that applications development work be initiated to apply HGMS to processes involving water or liquid slurries of coal. There are many of these applications. For example water slurries of coal fines are found in mine mouth coal cleaning operations and in pipe line transport of coal. Coal in oil dispersions for firing boilers and coal in various organic liquids are found in the initial steps of coal liquifaction processes.

REFERENCES

1. S. Siddiqui, Desulfurization and Concentration of Coal, German Patent 1,005,012, March 28, 1957.

2. S. Siddiqui, Recovery of Coal Resins with Partial Desulfurization of Coal, U.S. Patent 2,272,265, November 27, 1956.

3. A. Yurovsky and I. Remesnikov, "Thermomagnetic Method of Concentrating and Desulfurizing Coal," Coke and Chemistry, Vol. 12, 1958, p. 8.

4. W. Kester, "Magnetic Demineralization of Pulverized Coal," Mining Engineering, Vol. 17, No. 5, 1965, p. 72.

5. A.H. Fine, M. Lowry, L.F. Power and G.H. Geiger, "A Proposed Process for the Desulfurization of Finely Divided Coal by Flash Roasting and Magnetic Separation," IEEE Trans. on Magn., Vol. MAG-12, 1976, p. 523.

6. W. Kester, "The Effect of High Intensity Magnetic Cleaning on Pulverized, High Sulfur, Bituminous Coals," Thesis, West Virginia University School of Mines, 1966.

7. R.D. Harris, "Reducing the Sulfur Content of Steam Coal by Removing Fine Iron Pyrite at the Power Station," Fall Meeting, Society of Mining Engineers of AIME, Phoenix, Arizona, October 7-9, 1965.

8. W. Kester, J. Leonard, and E. Wilson, "Reduction of Sulfur from Steam Coal by Magnetic Methods," Mining Congress Journal, Vol. 53, No. 7, 1967, p. 70.

9. S.C. Trindade, "Studies on the Magnetic Demineralization of Coal," Massachusetts Institute of Technology Dissertation No. 1329, April 1973.

10. S. Trindade and H.H. Kolm, "Magnetic Desulfurization of Coal," IEEE Trans. on Magn., Vol. MAG-9, 1973, p. 310.

11. S. Trindade, J.B. Howard, H.H. Kolm, and G.J. Powers, Fuel, Vol. 53, No. 3, 1974, p. 178.

12. Proceedings of the High Gradient Magnetic Separation Symposium, edited by J. Oberteuffer and D. Kelland, Massachusetts Institute of Technology, Francis Bitter National Magnet Laboratory, June 22, 1973.

13. J. Oberteuffer, "High Gradient Magnetic Separation," IEEE Trans. on Magn., Vol. MAG-9, 1973, p. 303.

14. H.H. Murray, "Beneficiation of Selected Industrial Minerals and Coal by High Intensity Magnetic Separation," IEEE Trans. on Magn., Vol MAG-12, 1976, p. 498.

15. C.J. Lin, Y.A. Liu, D.L. Vines, M.J. Oak, G.E. Crow, and E.L. Huffman, "Studies on Sulfur Recovery from Coal Wastes and Prospective Magnetic Separation Applications," IEEE Trans. on Magn., Vol. MAG-12, 1976, p. 513.

16. E. Cohen and J. A. Good, "The Application of a Superconducting Magnet System to the Cleaning and Desulfurization of Coal," IEEE Trans. on Magn., Vol. MAG-12, 1976, p. 503.

17. Y. A. Liu and C. J. Lin, "Assessment of Sulfur and Ash Removal from Coals by Magnetic Separation," IEEE Trans. on Magn., Vol. MAG-12, 1976, p. 538.

18. R. R. Oder, "High Gradient Magnetic Separation Theory and Applications," IEEE Trans. on Magn., Vol. MAG-12, 1976, p. 428.

19. C. P. Bean, Bull. Am. Phys. Soc., Vol. 16, 1971, p. 350.

20. J. H. P. Watson, J. Appl. Phys., Vol. 44, 1973, p. 4209.

21. G. Zebel, J. Colloid Science, Vol. 20, 1965, p. 522.

22. J. A. Oberteuffer, IEEE Trans. on Magn., Vol. MAG-9, Sept. 1973, pp. 303-306.

23. J. A. Oberteuffer, Proceedings of the High Gradient Magnetic Separation Symposium, May 22, 1973, edited by J. A. Oberteuffer and D. Kelland, Massachusetts Institute of Technology, Francis Bitter National Magnet Laboratory, June 27, 1973.

24. C. P. Bean, Bull. Am. Phys. Soc., Vol. 16,1971, p. 350 and in more detail in personal notes.

25. J. H. P. Watson, J. Appl. Phys., Vol. 44, Sept. 1973, pp. 4209-4213.

26. G. Zebel, J. Colloid Science, Vol. 20, 1965, pp. 522-543.

27. D. Himmelblau, "Observation and Modeling of Paramagnetic Particle Trapping in a Magnetic Field," Massachusetts Institute of Technology, Masters thesis, June 1973.

28. C. Cowen, F. Friedlaender, and R. Jaluria, IEEE Trans. on Magn., Vol. MAG-12, 1976, p. 898.

29. F. E. Luborsky and B. J. Drummond, IEEE Trans. on Magn., Vol. MAG-11, 1975, p. 1696.

30. Electrochemistry of Cleaner Environments, edited by J. O'M. Bockris (Plenum Press, N. Y., 1972), Chapter 5 by E. C. Potter, p. 138.

31. F. E. Luborsky and B. J. Drummond, IEEE Trans. on Magn., Vol. MAG-12, 1976, p. 463.

32. H. Schlichting, Boundary Layer Theory (McGraw-Hill Co., Inc., New York, 1960), Chap. XII.

33. C. Cowen, F. J. Friedlaender, and R. Jaluria, IEEE Trans. on Magn., Vol. MAG-11, 1975, p. 1600.

34. E. Maxwell and D. Kelland, "Matrix Loading in High Gradient Magnetic Separators," Digests of INTERMAG Conf., 1975, IEEE Pub. 75CHO 932-4-MAG, Paper No. 24-5.

35. W. F. Lawson, Jr. "The Dynamics of Paramagnetic Particles Near a Magnetized Wire," Thesis, West Virginia Univ., Morgantown W. VA., 1976.

36. J. F. Lefelhocz, R. A. Friedel, and T. P. Kohman, "Mössbauer Spectroscopy of Iron and Coal," Geochimica Cosmochimica Acta, Vol. 31, 1967, pp. 2261-73.

37. T. P. Kohman et al., USAEC Report NYO-844-81, II. A. 4., 30 June 1970, pp. 31-34; USAEC Report COO-3236-3, II. A. 1, 31 May 1972, pp. 5-16.

38. L. F. Vassamillet, Proc. Seventh Nat. Conf. on Electron Probe Analysis, San Francisco, CA., 17-21 July 1972.

Appendix A

TYPICAL COMPUTER PROGRAM TO CALCULATE PERFORMANCE OF A HIGH GRADIENT MAGNETIC SEPARATOR

```
•OLD FE12B16
•RUN
•  ST

1000 LET P=0
1010 LET H=5E+3
1020 GO TO 1180
1030 IF H>80E+3 THEN 3340
1040 IF H>60E+3 THEN 1170
1050 IF H>40E+3 THEN 1150
1060 IF H>20E+3 THEN 1130
1070 IF H>10E+3 THEN 1110
1080 IF H>1E+3 THEN 1090
1090 LET H=10.69E+3
1100 GO TO 1180
1110 LET H=21.38E+3
1120 GO TO 1180
1130 LET H=42.75E+3
1140 GO TO 1180
1150 LET H=64.13E+3
1160 GO TO 1180
1170 LET H=85.5E+3
1180 LET V2=1.51
1190 IF V2=1.51 THEN 1330
1200 LET V2=1.74
1210 GO TO 1330
1220 LET V2=2.8
1230 GO TO 1330
1240 LET V2=2.98
1250 GO TO 1330
1260 LET V2=3.26
1270 GO TO 1330
1280 LET V2=4.55
1290 GO TO 1330
1300 LET V2=5.86
1310 GO TO 1330
1320 LET V2=9.8
1330 IF P=0 THEN 1430
1340 IF P=.002 THEN 1430
1350 IF P=.011 THEN 1400
1360 IF P=.011 THEN 1370
1370 LET P=.002
1380 LET A1=.004
1390 GO TO 1450
1400 LET P=.011
1410 LET A1=.02
1420 GO TO 1450
1430 LET P=.022
1440 LET A1=.04
1450 LET R6=0
1460 LET D3=1
1470 LET D1=5
1480 LET C1=.0032
1490 LET S=.01
1500 LET N=1416
1510 LET L=11.9
1520 LET P=.1
1530 LET S2=149.8
1540 LET L1=L/10
1550 LET P1=1
1560 LET P2=0
1570 LET D2=7.86
1580 LET X0=-.7E-6
1590 LET X1=1.075/H+10E-6
1600 LET X2=-.6E-6
1610 LET X=P1*X1+P2*X2-X0
1620 LET T=.058
1630 LET I=.074
1640 LET D7=1
1650 LET V3=(8*3.14*X*H*H*P^2)/(9*S*A1)
1660 IF H<7500 THEN 1680
1670 GO TO 1690
1680 LET V3=(V3*H)/(2*3.14*M)
1690 LET R9=0
1700 PRINT
1710 PRINT USING 1740,"FIBER EFFIC.=";C1;"MECH.ADJ.=";D7
1720 PRINT USING 1750,"FIBER RAD.=";A1;"WIDTH=";S
1730 PRINT USING 1760,"THICKNESS=";T
```

Reproduced from
best available copy.

```
1740:"LLLLLLLLLLLLLLa.aaaaaa              "LLLLLLLLLLa.aaaaaa
1750:"LLLLLLLLLLLLLLa.aaaaa               "LLLLLLLLa.aaaa
1760:     LLLLLLLLLLa.aaaaa
1770 PRINT
1780 PRINT
1790 PRINT "APPLIED FIELD=";H
1800 PRINT USING 1820,"ENTR.VELOCITY=";V2;"MAG.VELOCITY=";V3
1810 PRINT USING 1830,"VM/V=";V3/V2
1820:"LLLLLLLLLLLLLaaa.aaa     "LLLLLLLLLLLLLaaaaaa.a
1830:     "LLLLLaaaaaa.a
1840 PRINT
1850 LET W0=0
1860 LET P1=0
1870 IF P=.011 THEN 1910
1880 IF P=.002 THEN 1910
1890 LET W1=2.295
1900 GO TO 1920
1910 LET W1=1.1475
1920 LET W6=W1
1930 IF P=.011 THEN 1970
1940 IF P=.002 THEN 1970
1950 LET D0=76.45
1960 GO TO 1980
1970 LET D0=33.225
1980 LET D2=D0
1990 LET I=-1
2000 IF I<0 THEN 2020
2010 LET W4=(P1*W0)+(P1*W1)
2020 GO TO 2040
2030 LET W4=W4+(P1*W1)
2040 LET W0=W1
2050 LET P4=0
2060 LET D1=D0
2070 LET B2=D7*(T+2*P)-(M1*Z*V2)
2080 LET B3=(-C1*P*L1*B2)/(3*S)
2090 LET P1=0
2100 LET I=I+1
2110 LET Z=0
2120 IF I<3 THEN 2140
2130 IF I<9 THEN 2250
2140 PRINT "I=";I;"  ";"DIAMAG.IN=";D1;"  ";"PARAMAG.IN=";W0
2150 PRINT
2160 GO TO 2250
2170 PRINT "I";TAB(4);"N";
2180 PRINT TAB(11);"P";
2190 PRINT TAB(19);"W2";
2200 PRINT TAB(28);"W1";
2210 PRINT TAB(39);"W3";
2220 PRINT TAB(48);"Z";
2230 PRINT TAB(57);"P4";
2240 PRINT TAB(66);"W8"
2250 LET N=-1
2260 LET N=N+1
2270 LET R3=R4
2280 LET R7=R6
2290 LET B1=V3/(2*V2*(1+(2*N*P/A1))^2)
2300 LET Y=(-C1*P*L1*B1)/(3*S)
2310 LET R=(1-EXP(Y))
2320 LET P6=A1+((2*N+1)*P)
2330 LET P5=A1+2*N*P
2340 LET Z2=6*P^2*SQR(3.1416*S*V2^3*D3/P5)*(1+(P5^2/P4^2))
2350 LET Z4=(16*3.1416^2*P^3*X*M*H*A1^2)/(3*P4^3)
2360 LET Z3=Z2/(2*Z4)
2370 IF Z3=1 THEN 2400
2380 IF Z3>1 THEN 2400
2390 GO TO 2410
2400 LET Z3=1
2410 LET Z1=(SQR(1-Z3^2))/Z3
2420 LET Z=ATN(Z1)
2430 LET W3=3.14*P*(T+2*(1+2*N)*P)*I2*L1*D1/(3*D2*I*T*L)
2440 LET W3=(W3*C1)
2450 LET W2=R*W1
2460 IF W2<W3 THEN 2480
2470 LET W2=W3
2480 IF Z>.7854 THEN 2530
2490 LET R3=((3.1416-4*Z)/3.1416)*W2
2500 LET P4=W8
2510 IF N=0 LET P6=W8
2520 GO TO 2540
2530 LET R3=0
2540 LET W8=W2-R3
2550 LET P4=R3+R3
2560 LET P6=R3+R7
2570 LET W1=W1-W2+R3
2580 GO TO 2690
2590 PRINT USING 2630,I,N,INT(10^4*P+.5)/10^4,INT(10^4*W2+.5)/10^4;
2600 PRINT USING 2660,INT(10^4*W1+.5)/10^4;
2610 PRINT USING 2670,INT(10^4*W3+.5)/10^4;
2620 PRINT USING 2680,INT(10^1*(Z/.0174S)+.5)/10^1;
2630 PRINT USING 2670,INT(10^4*R3+.5)/10^4;
```

```
2640 PRINT USING 2670,INT(10^4*W8+.5)/10^4
2650:a  aaa  a.aaaa  a.aaaa
2660:    aaa.aaaa
2670:    aa.aaaa
2680:     aa.a
2690 LET R=.1
2700 IF W2/R*W9 THEN 2720
2710 GO TO 2260
2720 LET W1=W1-(R1*W0)
2730 LET O0=(O1-(R1*O1))
2740 LET W5=W0
2750 LET G0=(W6-W1)/((W6-W1)*(O2-O1+R1*O1))
2760 IF I=9 THEN 2780
2770 IF I<9 THEN 3010
2780 PRINT
2790 PRINT
2800 PRINT "Z2=";Z2,"P1=";P1,"P2=";P2
2810 PRINT "P=";P,"W6=";W6,"O2=";O2
2820 PRINT TAB(33);"SUMMARY"
2830 PRINT "LAST N=";N
2840 PRINT "INC.MAG.REC.FRAC.,=";(W0-W1)/W0;
2850 PRINT TAB(37);"INC.MAG.REC.WT.,=";(W0-W1)-(R1*W5)
2860 PRINT "MECH.REC.FRAC.,R1=";R1;
2870 PRINT TAB(37);"INC.MECH.REC.WT.,=";R1*W5
2880 IF W0<W6 THEN 2920
2890 PRINT "TOT.MECH.WT.REC.,=";(R1*W0);
2900 PRINT TAB(37);"TOT.MAG.WT.REC.=";(W6-W1)-(R1*W0)
 10 GO TO 2950
 20 PRINT "TOT.MECH.WT.REC.,W4=";W4;
2930 PRINT TAB(37);"TOT.MAG.WT.REC.=";(W6-W1)-W4
2940 PRINT "TOT.MAG.+MECH.REC.WT.=";(W6-W1)
2950 PRINT "TOT.MAG.+MECH.REC.,%=";(W6-W1)*100/W6;
2960 PRINT TAB(37);"GRADE,G0=";G0
2970 PRINT "DIAMAG.OUT,Q0=";Q0;
2980 PRINT TAB(37);"PARAMAG.OUT,W1=";W1
2990 PRINT "TOTAL SWEPT OFF,R6=";R6;TAB(37);"INC.SWEPT OFF,R4=";R4
3000 PRINT
3010 LET Y8=(W6-W1)
3020 IF P<.022 THEN 3040
3030 GO TO 3050
3040 LET Y8=Y8+Y6
3050 IF W0<W6 THEN 3080
3060 LET Y9=(W6-W1)-(R1*W0)
3070 GO TO 3090
3080 LET Y9=(W6-W1)-W4
3090 IF P=.011 THEN 3130
3100 IF P=.002 THEN 3150
3110 LET P9=100*Y9/17.5
3120 GO TO 3160
3130 LET P8=100*Y9/17.5
3140 GO TO 3160
3150 LET P7=100*Y9/17.5
3160 IF I<9 THEN 3210
  0 PRINT ".5*W1,%R=";P9;TAB(30);".25*W1,%R=";P8;TAB(55);".25*W1,%R=";P7
3180 PRINT "R7,GMS.=";Y8,"%R7=";100*Y8/17.5
3190 LET Y6=Y8
3200 IF I=9 THEN 3230
3210 RESTORE
3220 GO TO 2000
3230 IF P=.002 THEN 3260
3240 IF P=.011 THEN 1370
3250 IF P=.022 THEN 1400
3260 IF V2=9.8 THEN 1030
3270 IF V2=5.86 THEN 1320
3280 IF V2=4.55 THEN 1300
3290 IF V2=3.26 THEN 1280
3300 IF V2=2.98 THEN 1260
3310 IF V2=2.8 THEN 1240
3320 IF V2=1.74 THEN 1220
3330 IF V2=1.51 THEN 1200
3340 END

READY

*BYE
**RESOURCES USED $   1.21, USED TO DATE $    1.21=  0%
**TIME SHARING OFF AT  10.287 ON  10/13/76
```

HGMS PROGRAM PRINT-OUT MANIPULATIONS

GTSS SYSTEM

PROGRAM NAME: FES2B1G

The program as saved will print standard calculations for all velocities and drive fields at I = 9 and last N.

To print both I = 0 through I = 9 and N = 0 through last N, at all velocities and drive fields, adjust program as follows: (longest possible print-out)

LINE NUMBER	CHANGE FROM:	CHANGE TO:
2130	IF I<9 THEN 2250	OMIT
2160	GO TO 2250	OMIT
2580	GO TO 2690	OMIT
2770	IF I<9 THEN 3010	OMIT
3160	IF I<9 THEN 3210	~~OMIT~~ REM

To print I = 0 through I = 9 for last N only, adjust program as follows:

LINE NUMBER	CHANGE FROM:	CHANGE TO:
2130	IF I<9 THEN 2250	OMIT
2770	IF I<9 THEN 3010	OMIT
3160	IF I<9 THEN 3210	~~OMIT~~ REM

To print any of the previous combinations at only one velocity, for example, V2 = 8 cm/sec. Adjust the program as follows:

LINE NUMBER	CHANGE FROM:	CHANGE TO:
1180	LET V2=1.51	LET V2=8
1190	IF V2=1.51 THEN 1330	IF V2=8 THEN 1330
3260	IF V2=9.8 THEN 1030	IF V2=9.8 THEN 1030

To print any of the previous combinations at only one drive field, for example, H = 62,000 Oe. Adjust the program as follows:

LINE NUMBER	CHANGE FROM:	CHANGE TO:
1010	LET H=5E+3	LET H=62E+3
1030	IF H>80E+3 THEN 3340	IF H=62E+3 THEN 3340

Appendix B

HIGH GRADIENT MAGNETIC SEPARATION FOR REMOVAL OF SULFUR FROM COAL

F.E. Luborsky

Supplement to Final Report

Period Covered: February 1 through July 15, 1977

Contract No. HO366008

BUREAU OF MINES
U.S. DEPARTMENT OF THE INTERIOR
PITTSBURGH, PENNSYLVANIA

September 19, 1977

General Electric Company
Corporate Research and Development
Schenectady, New York

FOREWORD

The work on this project was accomplished by Corporate Research and Development personnel of the General Electric Company (Schenectady, N.Y.) with the leadership of F.E. Luborsky; by the personnel of the Francis Bitter National Magnet Laboratory of the Massachusetts Institute of Technology (Cambridge, Mass.) with the leadership of E. Maxwell; and by personnel of the Eastern Associated Coal Corp. (Everett, Mass.) with the leadership of H.E. Harris.

TABLE OF CONTENTS

Section		Page
I	Summary	B-1
II	Objective	B-1
III	Background	B-1
IV	Experimental Apparatus	B-1
V	Coal Sample	B-3
VI	Sample Size	B-3
VII	Analysis Procedure	B-4
VIII	Results	B-5
IX	Conclusions	B-14
X	Recommendations	B-15

LIST OF ILLUSTRATIONS

Figure		Page
1	Dry Separation Apparatus	B-2
2	Eschka-Leco Correlation	B-5
3(a)	Dry Separation. Sulfur and Ash Reduction as Function of Recovery, Delmont 7945	B-10
3(b)	Dry Separation. Sulfur and Ash Reduction as Function of Recovery, Delmont 8118	B-10
4	Wet Separation. Sulfur and Ash Reduction as Function of Recovery for Delmont 7945	B-11
5	Cumulative Reduction in Sulfur and Ash for Run 11	B-13
6	Wet Separation. Sulfur and Ash Reduction as Function of Field for Delmont 7945	B-14

LIST OF TABLES

Table		Page
I	Dry Separations	B-6
II	Wet Separations	B-7
III	Dry Separation - Delmont 7945	B-8
IV	Wet Separation - Delmont 7945	B-9

I. SUMMARY

The removal of sulfur and ash from dry powdered coal by high gradient magnetic separation has been successful. The pyritic sulfur and ash reduction of the coal was equivalent to that obtained in water slurries, but the percentage of coal recovered was somewhat lower and lower throughputs were required. The removal of the coal fines and the vibration of the canister were both helpful in improving the separator performance.

Wet separations in methanol slurries were shown to be effective.

Tests on oxidized vs. fresh coal resulted in equivalent separations.

II. OBJECTIVE

This report covers the supplemental HGMS tests on Upper Freeport coal from the Delmont mine. The purpose of these tests was to get additional data on the dry separation of pyrite and ash from coal in an effort to gain a better understanding of why our earlier results on dry separation were unsatisfactory and how they might be improved.

III. BACKGROUND

The earlier tests (described in the Final Report of Contract No. HO366008, February 1977) were performed by injecting pulverized coal into a relatively high-velocity air stream, which was then passed through the separator in a manner analogous to that done with water slurries. The poor separations were thought to result from the agglomeration of coal and mineral particles. It was observed that the separation was marginally better when the fines were taken out, and it was hypothesized that fines promoted agglomeration. We also suspected that there might be significant turbulent flow in the neighborhood of individual matrix fibers, which would result in large viscous forces on the particles, possibly making the retention of trapped particles on the matrix very difficult. Electrostatic forces did not appear to be significant factors.

IV. EXPERIMENTAL APPARATUS

In the dry separation tests carried out in this supplementary program, we abandoned the use of an air stream for propelling the coal through the matrix and instead used gravity feed, assisted by vibration, to move the coal. A combination of mechanical and electromagnetic means was employed. These means are shown in Figure 1, which is a sketch of the experimental apparatus. The matrix canister and feed pipe were supported by a thick rubber diaphragm fastened to the feed pipe at the top of the magnet opening. This

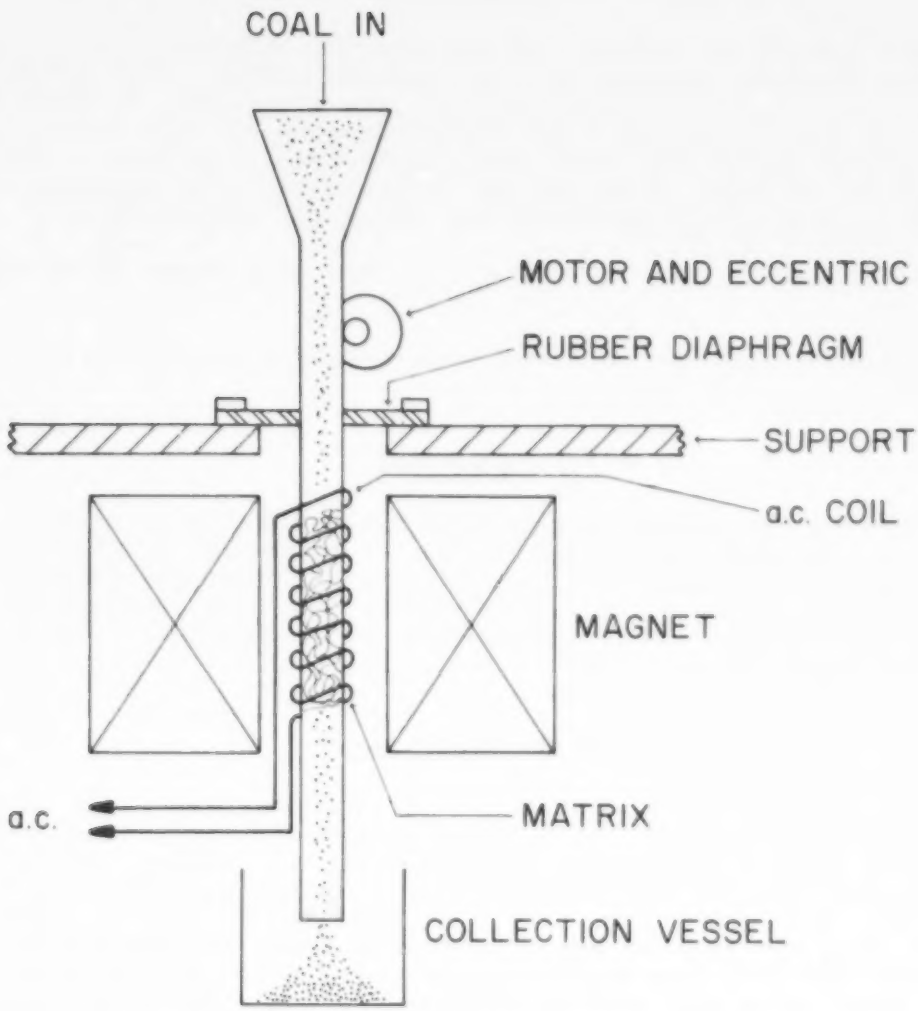

Figure 1. Dry Separation Apparatus

arrangement provided sufficient flexibility for both longitudinal and lateral vibration.

Lateral mechanical vibration was provided by an eccentric rotating shaft driven by a variable speed motor and positioned to strike the side of the feed pipe once per revolution. Longitudinal electromagnetic vibration was provided by a coil on the matrix canister energized with strong alternating current. A vibratory force was exerted on the coil by the interaction of the dc field of the magnet and the ac in the coil. No effort was made to quantify the amplitude of vibration in absolute terms, but the vibration was adjusted to permit relatively easy motion of the coal through the canister. The ac current through the coil was fixed, so the amplitude of this component of the vibration did change proportionately to the dc magnetic field.

V. COAL SAMPLE

The coal sample we used for most of the tests was taken from the same 60 mesh x 0 batch of Delmont 7945 coal used in the earlier series of tests. Tests at EAC indicated that the original lot, from which our sample had been prepared, had weathered significantly, with measurable conversion of pyrite to sulfate. Eastern's analysis as of June 27, 1977, was as follows:

Ash	14.6 %
Total sulfur	1.55%
Pyritic sulfur	0.75%
Sulfate sulfur	0.31%
Organic sulfur	0.49%

Late in the test period we did obtain a fresh sample of Delmont coal (#8118) from the mine and were able to carry out a few dry separations on it. The EAC analysis of this material was

Ash	16.0 %
Total sulfur	3.42%

No analysis of the forms of sulfur was made.

In addition to the dry tests we performed some wet separations. In view of the fact that the coal had probably undergone alteration since our earlier wet tests, this gave us a proper baseline for comparison with the dry tests. It was also useful to see, if possible, what effect sulfate conversion would have on magnetic separation.

We also carried out a few wet separations using methanol and methanol-water mixtures as the carrier fluid. The use of methanol avoids the necessity of drying the coal after magnetic separation. One can visualize a separation scheme in which a circulating load of methanol is used to carry the coal through the separator. Provided that the methanol losses could be kept small, this should be a workable technique which would combine the advantages of wet and dry separations. Methanol-water mixtures could also be useful if it turned out that drying would be significantly easier for some methanol-water proportion than for water alone.

VI. SAMPLE SIZE

These tests were conducted with relatively small feed samples of coal, of the order of 20 g in the dry tests and 80 g in the wet tests. One reason for these small samples was that, because we had a limited supply of the prepared coal on hand in our laboratory and because of the short time available for testing, we could not wait for the delivery of a fresh sample from the mine and its

preparation by EAC. Second, it was easier to do the dry tests with small samples; moreover, the mass materials balances were very good — of the order of 1%. Inasmuch as our main purpose was to investigate the factors which might inhibit or promote dry separation, rather than to simulate a large-scale process, there was no advantage in working with large samples.

VII. ANALYSIS PROCEDURE

Most of the ash and sulfur analyses of our test products were performed by EAC. In a few runs they determined the various forms of sulfur present, but for the remainder only total sulfur analyses were done. They analyzed some feed samples and the products (non-magnetics) of each run. The magnetics (mags) were not analyzed by them. Because of the tight time schedule, it was decided to concentrate on the product analyses.

We did carry out some total sulfur determinations in our own laboratory using the Leco apparatus. Initially we tested a few of the mags samples and later extended this to include non-mags samples as well. In cross-checking with the EAC determinations we found a systematic difference in total sulfur determinations between the EAC analyses by the Eschka method and ours by the Leco. (EAC informs us that their Pittsburgh laboratory has also observed systematic differences in the two methods.) In Figure 2 we show the results of such a correlation for 17 samples. The correlation between the two sets of observations, determined by a linear regression, is

$$S_{Eschka} = 1.0153\ S_{Leco} + 0.2396.$$

If the slope of the line were assumed equal to one, the least squares value of the intercept would be 0.2540.

A Leco standard sample (prepared by Leco) and rated as 2.45% sulfur was analyzed by the Eschka method; the analysis yielded a result of 2.68%.

Because we could hardly hope to completely resolve these discrepancies within the scope of the present investigation, we have referred all our data to the Eschka scale, which is the presently accepted standard in the coal industry. Leco analyses were then converted to equivalent Eschka values by means of the relation $S_{Eschka} = 1.0153\ S_{Leco} + 0.2396$. Where we present data taken with the Leco apparatus, we have already converted the values.

Because of the fact that our mass material balances were good, we calculated the percentage of sulfur in each feed, using the separate sulfur analysis data for mags and non-mags and assuming perfect sulfur materials balance. Alternatively we could have attempted to take a representative sample of each feed and analyzed it for sulfur. If we had been working with large samples, this method probably would have been preferable, but because we

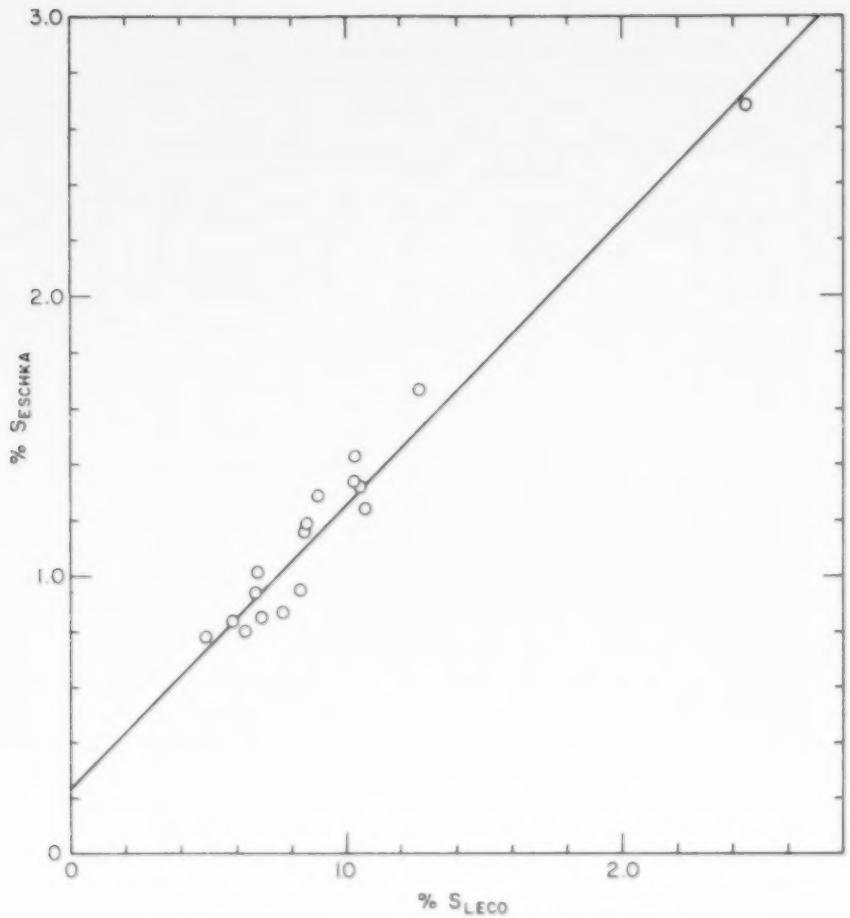

Figure 2. Eschka-Leco Correlation

used small samples in these tests, and in view of the good mass balance, the first approach probably has less error. In those cases where a product was analyzed by both the Eschka and Leco methods, we used the average figure, after adjusting the Leco value to the Eschka scale as explained above. There was generally good agreement between these separate determinations.

VIII. RESULTS

The scope of the experimental runs is set forth in Tables I and II for the dry and wet runs, respectively. More detailed data on these runs is given in Tables III and IV. In the dry separations the coal was fed into the system manually at a relatively slow rate to avoid the accumulation of a slug of coal which could clog the system. Tests were made at fields of 0 to 64.5. The coal sample available to us was a 60 mesh x 0 size distribution, and it was used in this form in several tests. We also separated some of this feed material in +200 mesh and -200 mesh size fractions and tested these separately. The non-mags fraction was captured by collecting the material that passed through the matrix with the field on and with

Table I - DRY SEPARATIONS

#	H kOe	Matrix	% Reduction Ash	% Reduction S	% Recov.	Vibration
			Delmont 7945			
2	20.0	ss wool	7.3	-1.5	90.8	both
3	20.0	"	3.0	-0.7	94.7	"
5	20.0	"	10.9	0.0	92.4	"
6	50.0	"	34.5	9.0	84.8	"
7	64.5	"	39.4	14.9	83.7	"
8	64.5	"	35.8	15.1	73.5	"
9	64.5	"	37.6	16.3	44.0	"
10	64.5	"	63.6	32.8	70.0	"
11	20.0	"	55.2	32.6	25.8	"
12	64.5	"	17.6	7.4	85.5	"
13	64.5	"	10.9	0.7	93.5	"
14	64.5	x-met[1]	72.7	42.9	52.0	e.m.
15	64.5	x-met	41.8	28.3	21.0	both
16	64.5	ss wool	33.3	9.1	61.0	both
17	50.0	"	26.1	7.6	81.5	e.m.
18	64.5	"		43.5	53.8	e.m.
19	20.0	"		33.6	54.9	mech.
20	64.5	"		38.0	67.5	"
21	20.0	"		12.9	87.6	"
22	64.5	"		25.2	49.0	"
23	0.0	"		-10.7	88.1	"
24	64.5	"		19.0	61.4	"
25	0.0	"		0.0	98.0	"
26	64.5	"		29.7	68.3	"
27	64.5	"		23.7	28.7	e.m.
28	64.5	x-met				both
29	64.5	"		21.2	52.9	e.m.
30	64.5	"		34.9	21.8	both
31	64.5	"				"
32	64.5	"		18.2	43.2	"
			Delmont 8118			
33	20.0			9.4	94.2	both
35	64.5			54.4	57.5	e.m.
36	20.0			18.7	63.0	e.m.
37	64.5			41.1	71.5	e.m.
38	20.0			14.9	72.0	e.m.
39	0.0			-0.7	80.0	none
40	0.0			-0.9	97.0	e.m.

Notes: 1. Expanded metal

Table II - WET SEPARATIONS

#	H kOe	V cm/s	Size	% Reduction Ash	% Reduction S	% Recov.	Medium
				Delmont 7945			
1W	64.5		60x0	47.9	22.0	67.8	W[1]
2W	50.0		60x0	48.4	29.9	74.0	W
3W	40.0		60x0	49.1	30.4	75.4	W
4W	20.0		60x0	33.3	17.8	83.8	W
5W	0.0		60x0	11.5	8.3	91.3	W
6W	64.5		60x0	52.7	32.3	66.2	W
7W	64.5		60x0	54.5	32.5	69.7	M[2]
8W	20.0		60x0	44.2	28.0	78.4	M
8W	0.0		60x0	6.1	4.1	92.7	M
10W	64.5		60x0	49.1	26.0	73.7	25% M
11W	64.5		+200	70.9	40.6	65.7	W
12W	20.0		+200	49.7	31.5	76.8	W
13W	64.5		60x0	50.3	35.5	71.7	10% M
14W	20.0		60x0	41.2	31.5	80.1	10% W
15W	64.5		60x0	49.1	27.4	76.1	50% M
16W	20.0		60x0	38.2	14.5	82.7	50% M
17W	64.5		60x0	58.8	35.5	67.7	M
18W	20.0		60x0	48.5	29.0	76.8	M
19W	64.5		60x0	47.3	37.1		M

Notes:

1. Water
2. Methanol

Table III - DRY SEPARATION - DELMONT 7945

#	Weight in Grams					% Total Sulfur					% Red. S	% Ash		% Red. Ash	% Recovery	H kOe	Size Fraction
	Prod.	Mags.	Residue	Σ	Feed	Eschka Product	Leco Product	Mags.	Residue	Feed		Prod.	Feed				
2	17.98	0.68	0.48	19.14	19.80	1.38		1.88	1.60	1.36	- 1.5	15.3	16.5	7.3	90.8	20.0	60 x 0
3	18.93	0.37	0.30	19.6	20.0	1.38		2.12	1.79	1.37	- 0.7	16.0		3.0	94.7	20.0	60 x 0
5	18.47	0.71	0.33	19.51	20.0	1.36		1.99	1.76	1.36	0.0	14.7		10.9	92.4	20.0	60 x 0
6	16.95	2.15	0.49	19.59	20.0	1.22		2.42	1.94	1.34	9.0	10.8		34.5	84.8	50.0	60 x 0
7	16.73	2.30	0.45	19.48	20.0	1.14		2.62	2.27	1.31	13.0	10.0		39.4	83.7	64.5	60 x 0
8	14.7	4.0	1.2	19.9	20.0	1.18		2.11	1.76	1.39	15.1	10.6		35.8	73.5	64.5	60 x 0
9	8.8	10.6	0.4	19.8	20.0	1.16	1.10	1.54	1.58	1.35	16.3	10.3		37.6	44.0	64.5	60 x 0
10	14.0	6.0	0.2	20.2	20.0	0.84	0.84	2.17	1.28	1.25	32.8	6.0		63.6	70.0	64.5	+200
11	a[1] 4.9	0.8	0.1	19.0	19.0	0.94	0.92	2.02	1.47	1.38	32.6	7.4		55.2	25.8	20.0	+200
	b[1] 4.6					1.32	1.31					13.4					
	c[1] 8.6					1.68	1.53					24.0					
12	17.1	2.4	0.7	20.2	20.0	1.34	1.29	1.99	1.65	1.42	7.4	13.6		17.6	85.5	64.5	-200
13	18.7	0.6	0.3	19.6	20.0	1.43	1.29	2.49	1.79	1.37	0.7	14.7		10.9	93.5	64.5	-200
14	10.2	9.3	1.0	20.5	19.6	0.78	0.74	1.80	1.53	1.38	44.9	4.5		72.7	52.0	64.5	+200
15	4.2	14.6	0.7	19.5	20.0	1.02	0.93	1.51	1.44	1.36	28.3	9.6		41.8	21.0	64.5	-200
16	12.2	7.6	0.3	20.1	20.0	1.19	1.32	1.56	1.41	1.38	9.1	11.0		33.3	61.0	64.5	60 x 0
17	16.3	3.0	0.5	19.8	20.0	1.29	1.15	1.88	1.86	1.32	7.6	12.2		26.1	81.5	50.0	60 x 0
18	6.4	5.6	0.1	12.1	11.9		0.87	2.25	1.43	1.54	43.5				53.8	64.5	+200
19	5.0	4.3		9.3	9.1		1.01	2.05		1.52	33.6				54.9	20.0	+200
20	8.1	3.7	0.1	11.9	12.0		0.88	2.64	1.49	1.42	38.0				67.5	64.5	+200
21	10.6	1.4	0.2	12.2	12.1		1.28	2.85	1.27	1.47	12.9				87.6	20.0	+200
22	5.0	5.1	0.1	10.2	10.2		1.13	1.88	1.41	1.51	25.2				49.0	64.5	60 x 0
23	8.9	0.0	0.2	9.1	10.1		1.55		1.48	1.40	-10.7				88.1	00.0	60 x 0
24	6.2	3.8	0.1	10.0	10.1		1.32	2.13	1.71	1.63	19.0				61.4	64.5	-200
25	9.8	0.0	0.2	10.0	10.0		1.64		1.46	1.64	0.0				98.0	00.0	-200
26	6.9	2.7	0.4	10.0	10.1		1.09	2.70	2.10	1.55	29.7				68.3	64.5	60 x 0
27	2.9	7.2		10.1	10.1		1.16	1.67		1.52	23.7				28.7	64.5	60 x 0
28																	
29	3.7	2.7	0.9	7.3	7.0	0.76	0.91	1.21	1.18	1.06	21.2				52.9	64.5	60 x 0
30	7.2	24.7	1.3	33.2	33.0	0.94	1.04	1.66	1.64	1.52	34.9				21.8	64.5	60 x 0
31	3.7	1.9	0.5	6.1	6.1			1.17	1.47						60.7	64.5	60 x 0
32	1.6	2.2	0.1	3.9	3.7	0.73	0.84	0.98	1.29	0.96	18.2				43.2	64.5	60 x 0

Notes: 1. Consecutive products: see text

Table III - DRY SEPARATION - DELMONT 7945 (Cont'd)

#	Weight in Grams				% Total Sulfur			% Red.	% Re-	H	Size
	Prod	Mags	Σ	Feed	Prod	Mags	Feed	S	covery	kOe	Fraction
33	20.0	3.3	23.3	21.24	3.47	3.64	3.83	9.4	94.2	20.0	60 x 0
35	11.5	9.1	20.6	20.0	2.31	8.23	5.07	54.4	57.5	64.5	+200
36	12.6	7.7	20.3	20.0	4.05	6.30	4.98	18.7	63.0	20.0	+200
37	14.3	5.7	20.0	20.0	2.85	9.84	4.84	41.1	71.5	64.5	+200
38	14.4	5.6	20.0	20.0	4.10	6.67	4.82	14.9	72.0	20.0	+200
39	16.0	3.1	19.1	20.0	4.37	5.47	4.34	-0.7	80.0	0.0	+200
40	19.8	0.5	20.3	20.42	3.45	3.06	3.42	-0.9	97.0	0.0	60 x 0

Table IV - WET SEPARATION - DELMONT 7945

#	Weight in Grams				% Total Sulfur				% Red.	% Ash		% Red.	% Re-	H	Size	Medium
	Prod	Mags	Σ	Feed	Eschka Leco Product		Mags	Feed	S	Prod	Feed	Ash	covery	kOe	Fraction	
1W	54.57	24.85	79.46	80.5	0.84	0.97	1.76	1.16	22.0	8.60	16.5[2]	47.9	67.8	64.5	60 x 0	W[3]
2W	60.79	21.68	82.47	82.1	0.77	0.94	2.24	1.22	29.9	8.52		48.4	74	50.0	60 x 0	W
3W	63.76	19.25	83.01	84.6	0.75	0.85	2.39	1.15	30.4	8.40		49.1	75.4	40.0	60 x 0	W
4W	69.38	12.28	81.66	82.8	0.91	1.03	2.47	1.18	17.8	11.0		33.3	83.8	20.0	60 x 0	W
5W	79.26	6.42	85.68	86.8	1.05	1.15	2.65	1.20	8.3	14.6		11.5	91.3	0.0	60 x 0	W
6W	59.78	29.11	88.89	90.3	0.80	0.88	2.12	1.24	32.3	7.8		52.7	66.2	64.5	60 x 0	W
7W	60.54	25.47	86.01	86.8	0.87	1.02	2.53	1.40	32.5	7.5		54.5	69.7	64.5	60 x 0	M[4]
8W	72.86	19.07	91.93	92.9	0.95	1.08	2.84	1.41	28.0	9.2		44.2	78.4	20.0	60 x 0	M
9W	75.58	5.65	81.23	81.5	1.24	1.33	2.10	1.34	4.1	15.5		6.1	92.7	0.0	60 x 0	M
10W	57.89	17.41	75.30	78.6	0.85	0.94	2.50	1.21	26.0	8.4		49.1	73.7	64.5	60 x 0	25% M
11W	40.27	19.52	59.79	61.3	0.66	0.79	2.35	1.22	40.6	4.8		70.9	65.7	64.5	+200	W
12W	43.77	12.09	55.86	57.0	0.75	0.88	2.68	1.19	31.5	8.3		49.7	76.8	20.0	+200	W
13W	55.03	20.02	75.05	76.7	0.80			1.24[1]	35.5	8.2		50.3	71.7	64.5	60 x 0	10% M
14W	62.88	13.01	75.89	78.5	0.85				31.5	9.7		41.2	80.1	20.0	60 x 0	10% M
15W	65.26	19.63	84.89	85.8	0.90				27.4	8.4		49.1	76.1	64.5	60 x 0	50% M
16W	66.64	13.59	80.23	80.6	1.06				14.5	10.2		38.2	82.7	20.0	60 x 0	50% M
17W	57.79	25.62	83.41	85.3	0.80				35.5	6.8		58.8	67.7	64.5	60 x 0	M
18W	62.47	18.40	80.87	81.3	0.88				29.0	8.5		48.5	76.8	20.0	60 x 0	M
19W	40.64[5]	12.73	53.37	67.2	0.78				37.1	8.7		47.3		64.5	60 x 0	M

Notes:

1. Average feed analysis for runs 1W-12W used for runs 13W-MW
2. EAC ash analysis of feed used throughout
3. Water
4. Methanol
5. Partial Product

vibration of the matrix. The mags fraction was collected by turning the field off and vibrating the matrix more vigorously. Finally, a residual mags fraction was collected by removing the matrix canister and rapping out the remaining few tenths of a gram of trapped material.*

The wet separations were carried out in the usual way (cf. volume 1 of this report) using water, methanol, and water-methanol mixtures. The product slurries collected were then filtered with a pressure filter to recover the dry products.

Figures 3(a), 3 (b), and 4 summarize the results of these tests. In these figures we have plotted (on a weight basis) the

*This represents a normal equilibrium buildup, which would level off in successive tests.

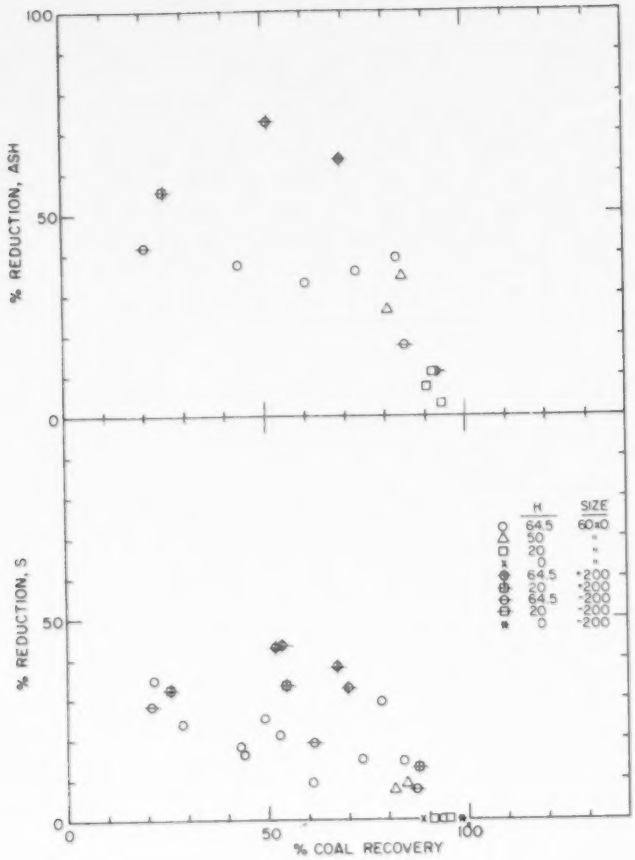

Figure 3(a). Dry Separation. Sulfur and Ash Reduction as Function of Recovery, Delmont 7945

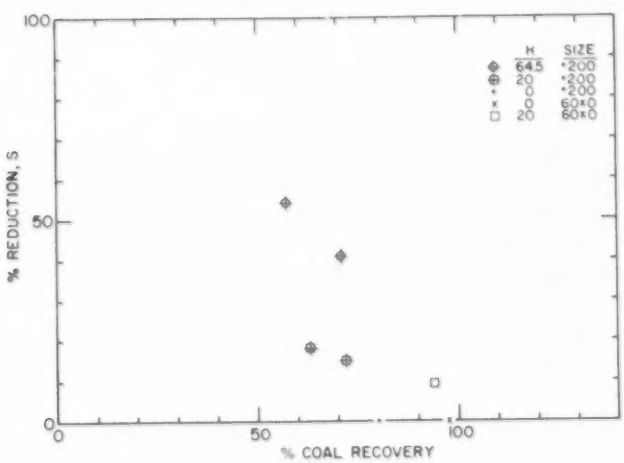

Figure 3(b). Dry Separation. Sulfur and Ash Reduction as Function of Recovery, Delmont 8118

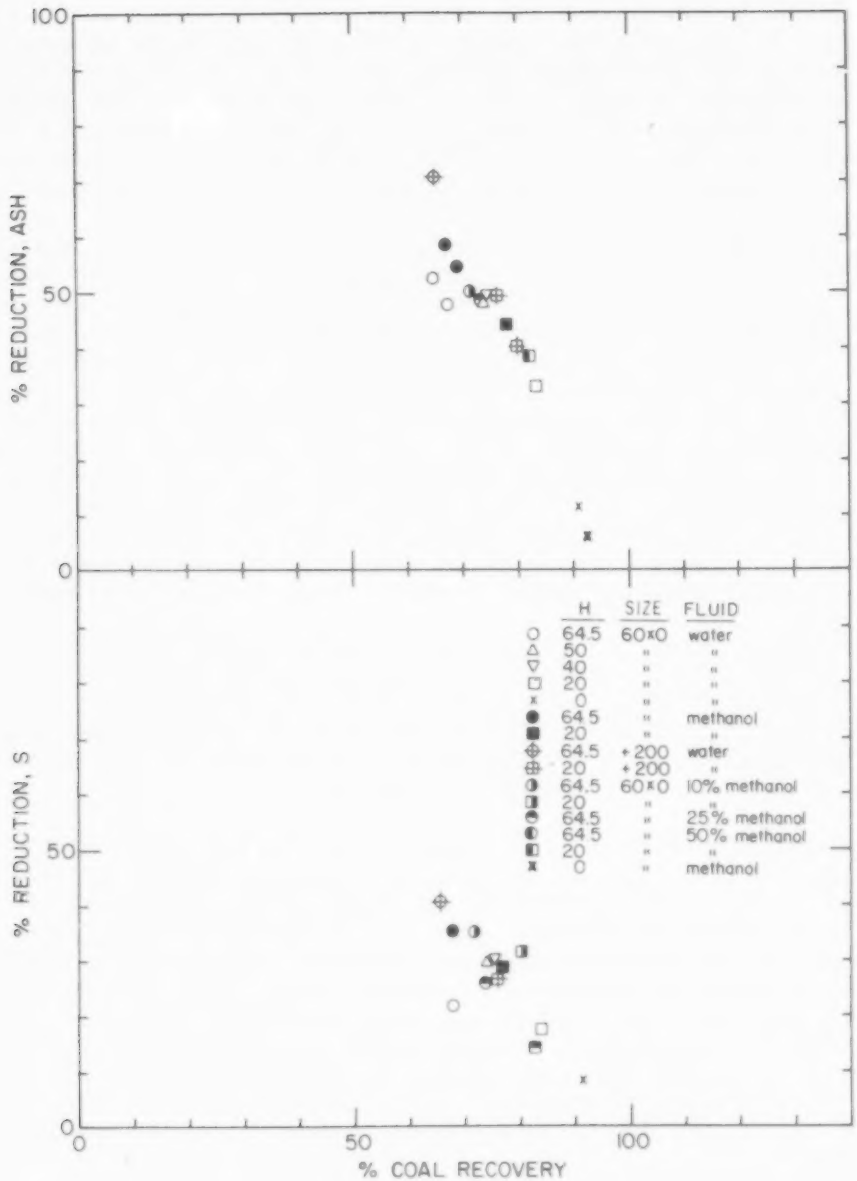

Figure 4. Wet Separation. Sulfur and Ash Reduction as Function of Recovery for Delmont 7945

percentage reduction in ash or sulfur in the non-mags, compared to the feed, vs. the percentage of the feed recovered in the non-mags.

$$\text{Percentage reduction} = \left[1 - \frac{\text{\% ash/sulfur in non-mags}}{\text{\% ash/sulfur in feed}}\right]$$

These plots are similar to the grade-recovery plots used in mineral beneficiation. At 100% recovery there is zero improvement in the grade (reduction of ash or sulfur), while, as 100% grade is approached, the recovery becomes vanishingly small.

Figure 4 presents the results of the wet separations. The separations on the +200 mesh fractions result in higher reductions of ash and sulfur at some cost in coal recovery. The higher fields also consistently yield products with greater reductions and lower recoveries than lower fields. One could, however, draw single curves which would be fair approximations to all the data points.

The results of the dry separations are shown in Figure 3(a) and Figure 3(b). Here it is clear that a single curve would not serve to represent the data. The +200 mesh data points yield results significantly better than those for 60 mesh x 0 fraction, and these in turn are better than for -200 mesh fraction. Although the data points for each set of conditions are few, it is clear that they could not be even approximately represented by a single curve. It is significant, however, that the best results (those obtained with the +200 mesh fraction) are roughly the same for both the wet and dry separations. This fact suggests that dry separations should be feasible if the fines are split off and if a practical feeding scheme can be devised which sifts the coal through a matrix without using a high-velocity air stream (e.g., fluidized bed).

Fewer data were taken on the freshly mined Delmont 8118 coal. These, however, are in general agreement with the data on the weathered Delmont 7945. In fact, the results are a little better. This is strong evidence that the success of pyrite removal in magnetic separation is not principally the result of oxidation of the coal and would apply to freshly mined coal.

As mentioned earlier, we generally used a combination of longitudinal vibration, induced electromagnetically, and lateral mechanical vibration, generated by rapping on the feed pipe with an eccentric rotating shaft. The longitudinal vibration was probably effective in moving the coal through the matrix; the lateral mechanical vibration tended to prevent coal from accumulating at the top of the matrix. There is some evidence that the mags fraction may not be completely immobilized on the matrix but is slowed down by the magnetic forces, while the clean coal moves more rapidly and accumulates more quickly in the collection vessel. In Run II we collected three successive product fractions in the following manner:

Fraction a - no matrix vibration
Fraction b - electromagnetic vibration only
Fraction c - electromagnetic + mechanical vibration.

The sulfur and ash reductions for these fractions were as follows:

Fraction	Reduction, %			Cumulative % Reduction		Cumulative Recovery, %
	S	Ash		S	Ash	
a	32.6	55.2	a	32.6	55.2	25.8
b	4.7	18.8	a+b	19.4	37.6	50.0
c	-16.3	-45.5	a+b+c	2.2	-1.8	95.3

The cumulative reductions and recoveries for these fractions are shown graphically in Figure 5.

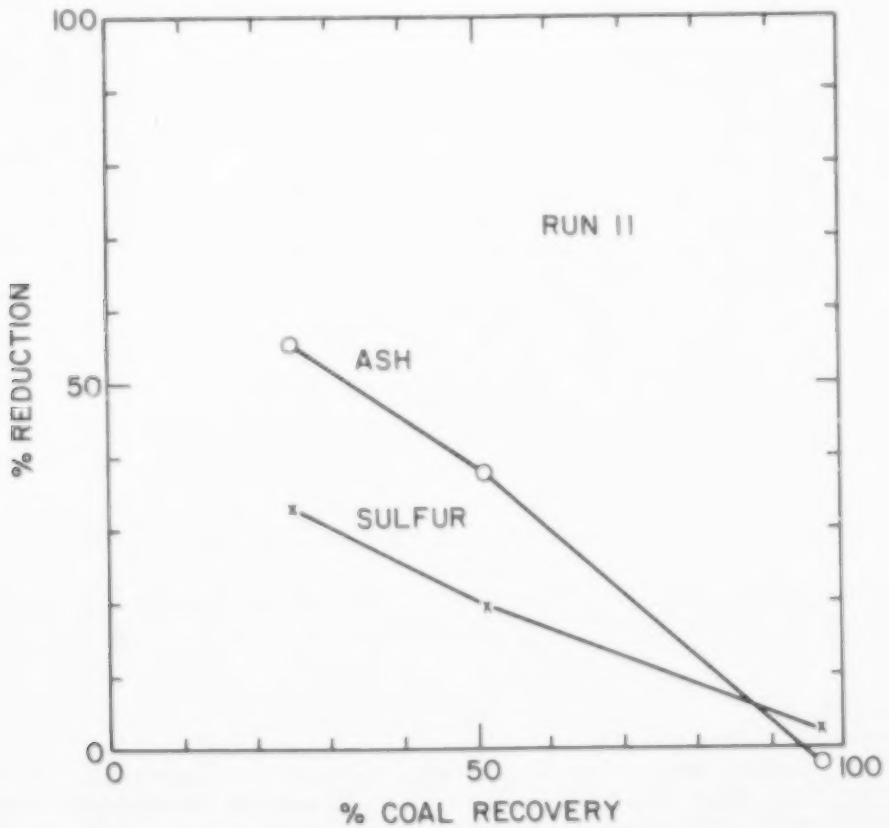

Figure 5. Cumulative Reduction in Sulfur and Ash for Run 11

In Figure 6 we show the percentage reductions in ash and sulfur for the wet separations vs. field strength. Higher reductions are obtained with +200 mesh fractions than with the 60 mesh x 0 size distribution. The separations in methanol are better than those in water; in methanol-water slurries the results fall in between. Methanol wets the coal easily and no dispersant is necessary,

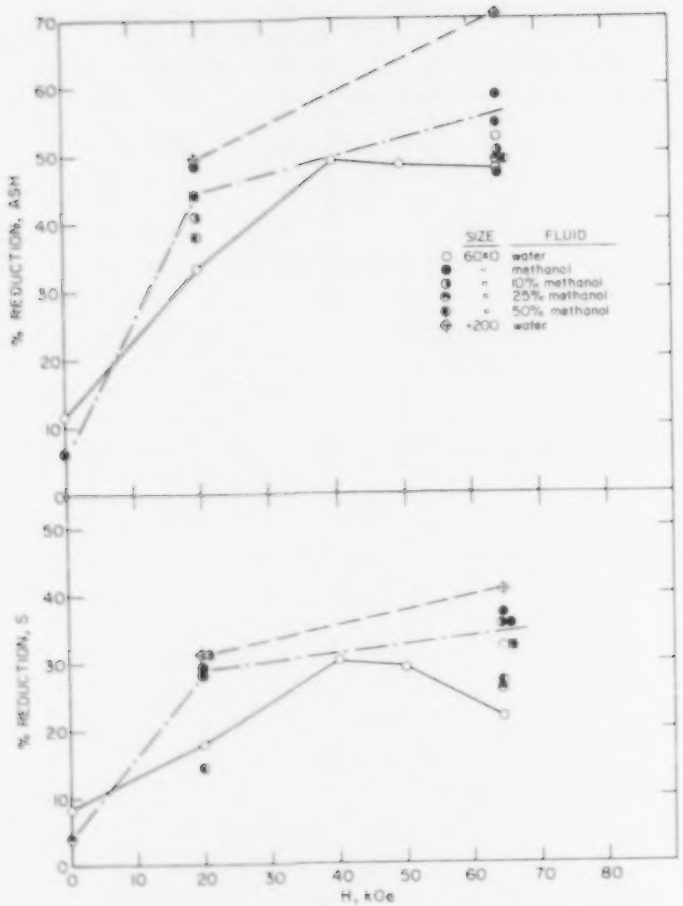

Figure 6. Wet Separation. Sulfur and Ash Reduction as Function of Field for Delmont 7945

even in the 10% methanol slurries. There is evidently less tendency for particles to agglomerate.

IX. CONCLUSIONS

1. Dry magnetic separation by HGMS should be feasible if the coal fines are separated out and if a suitable technique for gravity feeding can be developed. Multiple passes may be desirable to increase the coal recovery. (In this work only single passes were taken.)

2. Wet separation in methanol or in water-methanol mixtures is an interesting alternative process deserving further investigation. If the separations were done with a circulating load of methanol, the drying problem would be eliminated or, in the case of methanol-water mixtures, may be reduced. In the short time available we could not investigate this problem further.

3. Tests on oxidized coal and freshly mined coal indicate that the pyrite removal is substantially the same in both cases.

X. RECOMMENDATIONS

Based on the satisfactory cleaning of sulfur and ash from a water slurry of United States coal and the equally effective cleaning of dry powders of the same coal, we strongly recommend the continuation of this work. The following specific items of work should be undertaken.

1. On dry coal cleaning, work should continue toward development of a suitable feeding procedure to lead to maximum throughput and maximum cleaning. Fluidized bed techniques or a development of gravity feeding procedures are indicated as the direction for this work. This should lead to an initial evaluation of the economics of the dry cleaning of this coal.

2. On water slurries of coal, a variety of coals mined in the United States should be subjected to high gradient magnetic separation, using the same equipment and procedures. This will yield information on the variability of the cleaning of coals from different sources, which is necessary to form the basis for determining how generally this type of cleaning can be applied.

3. The variety of coals to be tested should be the same as that for dry powders.

4. Methanol and methanol-water slurries should be tested to see in detail how well the high gradient cleaning works as compared to water slurries. Further questions to be answered include the following: Are wetting agents or dispersants needed? Under what conditions, how efficiently, and how much energy is required to recover the methanol? This preliminary analysis should be sufficient to evaluate whether or not further work is justified.

5. Oil-coal slurries should also be evaluated because of their potential in power plant applications.

6. All of the above work should be closely coupled with continuing work on the fundamental understanding of the various aspects of the problem - for example: on developing better physical modeling for the magnetic separation in both wet and dry systems; on determining the mineral phases present, their physical and magnetic properties, their changes during processing, and means of enhancing their magnetic properties.